Journal of the Geological Society, London, Vol. **171**, 2014, pp. 425–441. http://dx.doi.org/10.1144/jgs2013-034
Published *Online First* on January 30, 2014

Evolution of a fault-controlled fissure-ridge type travertine deposit in the western Anatolia extensional province: the Çukurbağ fissure-ridge (Pamukkale, Turkey)

ANDREA BROGI[1*], ENRICO CAPEZZUOLI[2], MEHMET CIHAT ALÇIÇEK[3] & ANNA GANDIN[2]
[1]*University of Bari, Department of Earth and Geoenvironmental Sciences, Via Orabona, 4, 70125, Bari, Italy*
[2]*University of Siena, Department of Physics, Earth and Environmental Sciences, Via Laterina, 8, 53100, Siena, Italy*
[3]*University of Pamukkale, Department of Geology, 20070, Denizli, Turkey*
**Corresponding author (e-mail: andrea.brogi@uniba.it)*

Abstract: In recent decades various interpretations have been proposed to explain the evolution of fissure-ridge-type travertine deposits. In this paper, we discuss the relationships between fissure-ridges and brittle structures affecting their substratum, through a detailed analysis of an inactive fissure-ridge (near Çukurbağ) located in the Pamukkale geothermal area (western Turkey). The Çukurbağ fissure-ridge can be taken as a model as it offers an opportunity to examine its internal structure on the walls of a Roman quarry; in addition, this ridge has been studied by several researchers who have discussed the processes promoting the fissure-ridge evolution. The Çukurbağ fissure-ridge is composed of irregularly alternating travertine laminated facies (bedded travertine) crosscut into rather large lithons by subvertical crystalline veins (banded travertine). The relationships between bedded and banded travertine indicate that the banded veins are diachronous and migrated through time, suggesting a progressive fault zone enlargement in the footwall. Such a fault zone was characterized by polycyclic activity, with normal to transtensional kinematics, and was active during the latest Quaternary. We demonstrate that formation of banded veins is coeval with bedded travertine deposition and strictly depends on fault activity, therefore highlighting the fundamental role of travertine fissure-ridges in reconstructing palaeotectonic activity in a region.

Faults and related damage zones are the most ubiquitous and efficient conduits for fluid migration in the Earth's crust (Kerrich 1986; Caine *et al.* 1996; Curewitz & Karson 1997; Aydın 2000; Sibson 2000; Tripp & Vearncombe 2004; Nelson *et al.* 2009; Person *et al.* 2012). If faulting affects areas characterized by geothermal anomalies promoting hydrothermal systems, bedrock damage will give rise to a network of connected fractures enhancing permeability in the rock masses, which promotes circulation and upwelling of hydrothermal fluids (Sibson 2000; Bellani *et al.* 2004; Rowland & Sibson 2004), often triggered by CO_2 pressure fluctuation (Uysal *et al.* 2009) and seismic activity (Gratier *et al.* 2002; Becken *et al.* 2011; Becken & Ritter 2012).

In this background, thermal springs are found aligned along the traces of relevant faults and/or related fractures, often suggesting their geometrical attitudes (Curewitz & Karson 1997, and references therein). Such springs can deposit carbonate masses (Ford & Pedley 1996; Pentecost 2005; Gandin & Capezzuoli 2008; Pedley 2009; Capezzuoli *et al.* 2013) if the fluids are characterized by appropriate chemistry (i.e. bicarbonate-supersaturated fluids). In the same way, the location, age and geometry of travertine bodies can helpfully contribute to infer the structural and permeability features of the main tectonic element triggering fluid circulation (e.g. Altunel & Hancock 1993*a*,*b*; Faccenna *et al.* 1993; Hancock *et al.* 1999; Martinez-Diaz & Hernandez-Enrile 2001; Brogi & Capezzuoli 2009; Temiz & Eikenberg 2011). Among the travertine bodies deposited from hydrothermal fluids discharged from tectonically controlled thermal springs (Hancock *et al.* 1999), travertine fissure-ridges (Bargar 1978) are an attractive subject for study, as their shape and internal architecture can reveal much about the geometry and kinematics of the main structure hidden by the travertine body (e.g. Brogi & Capezzuoli 2009). Accordingly, fissure-ridges are useful morphotectonic features to locate faults and/or associated fractures occurring in areas affected by neotectonics and/or active tectonics.

Several fissure-ridges described around the world (Altunel & Hancock 1993*a*,*b*, 1996; Çakir 1999; Guo & Riding 1999; Atabey 2002; Altunel & Karabacak 2005; Yanik *et al.* 2005; Mesci *et al.* 2008, 2013; Brogi & Capezzuoli 2009; Selim & Yanik 2009; Temiz *et al.* 2009; Temiz & Eikenberg 2011; De Filippis & Billi 2012; De Filippis *et al.* 2012, 2013*a*,*b*) are straight or curvilinear in plan view and can be up to 2.5 km long, 400 m wide and 20–25 m high. A typical fissure-ridge (Fig. 1) consists of a triangular-shaped body made of bedded carbonates dipping away (from 5° to 90°) from a central fissure(s) running along its long axis. The central fissure(s) corresponds in depth to a bundle of veins ranging from some millimetres to a few metres in width, filled by vertical laminated palisade or fibrous calcite and/or aragonite (described as banded travertine by Altunel & Hancock 1993*a*,*b*). The veins come upwards from the bedrock, which is hidden below the bedded travertine. Banded travertine mainly develops on the walls of the fissure by upwelling thermal waters that afterwards flow out at the top of the ridge, promoting its progressive construction. Banded travertine can also grow as sill-like structures and injection veins (see Uysal *et al.* 2009; De Filippis *et al.* 2012), giving rise to a more or less complex vein network. Thus, the internal architecture of the ridge, its morphology (both in cross-section and in plan view), and banded–bedded travertine relationships can reveal much about the fissure-ridge evolution and brittle deformation affecting the substratum.

Although there is a general consensus that travertine fissure-ridges are tectonically controlled bodies, various mechanisms and growth processes have been proposed to explain their development. Concerning the mechanisms, some researchers have related fissure-ridges to progressive enlargement of dilatational fractures affecting the bedrock (Altunel & Hancock 1993*a*,*b*; Hancock *et al.* 1999; Mesci *et al.* 2008; Temiz *et al.* 2009); in contrast, others have demonstrated that travertine fissure-ridges are syntectonic deposits growing along tracts of fault traces (Altunel & Hancock 1996;

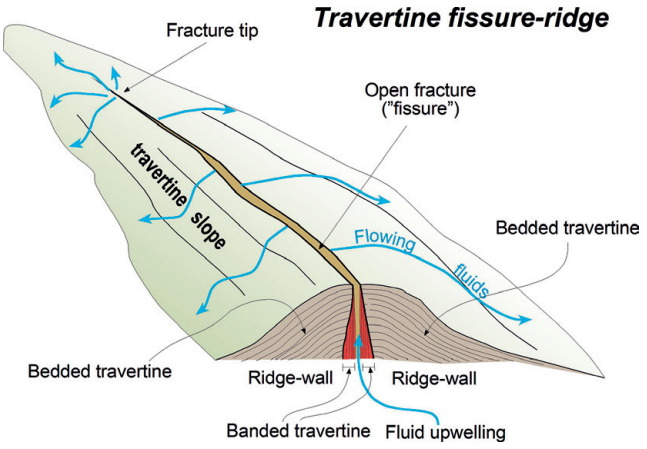

Fig. 1. Schematic illustration of the anatomy of a travertine fissure-ridge.

Brogi & Capezzuoli 2009). Concerning the growth processes, some workers have assumed that the coeval deposition of banded and bedded travertine is tectonically controlled and related to the progressive dilatation of the ridge (Altunel & Hancock 1993*a*,*b*; Çakir 1999; Mesci *et al.* 2008; Temiz & Eikenberg 2011), whereas others have suggested that banded and bedded travertine were deposited at different periods owing to the combined effects of climate, local subsidence and gravitational collapse of the ridge (De Filippis *et al.* 2013*a*,*b*). De Filippis *et al.* (2012, 2013*a*) hypothesized that fissure-ridges grew preferentially during warm and/or humid periods and were cut by axial veins and sill-like structures (banded travertine) during arid periods. In their hypothesis palaeoclimate oscillations must have controlled the amount of fluid discharge influencing the opening of the feeding fractures by an increased pore pressure.

With the aim of contributing to the better understanding of the processes promoting the growth of the travertine fissure-ridges and in an attempt to obtain a conceptual model for their development mechanism, the Çukurbağ fissure-ridge, located in the Pamukkale geothermal area (Fig. 2), western Turkey, has been examined in detail. Although many fissure-ridges and travertine bodies associated with active normal and strike-slip faults have been described for western Turkey (Altunel & Hancock 1993*a*, *b*; Çakır 1999; Hancock *et al.* 1999; Atabey 2002; Altunel & Karabacak 2005; Yanik *et al.* 2005; Mesci *et al.* 2008; Selim & Yanik 2009; Temiz *et al.* 2009; Kele *et al.* 2011; Temiz & Eikenberg 2011; De Filippis *et al.* 2012, 2013*a*,*b*), we deal with the Çukurbağ fissure-ridge, as it has been investigated by several researchers who have proposed different and contrasting hypotheses: it was considered to be (1) developed on a dilatational fracture (Altunel & Hancock 1996; Hancock *et al.* 1999), (2) induced by increasing pore pressure owing to climatic fluctuation (De Filippis *et al.* 2013*a*) or (3) deposited in a subsiding area related to its progressive weighting (De Filippis *et al.* 2012). In addition, the Çukurbağ fissure-ridge is inactive and was partially quarried during the Roman period (Fig. 3), therefore offering an opportunity to investigate its internal parts, which were uncovered by the excavation. For all these reasons this travertine body represents a key fissure-ridge for investigation.

Geological setting

The Çukurbağ fissure-ridge is part of the Quaternary, still active travertine body exposed in the Pamukkale geothermal field (near the ancient Roman town of Hierapolis), which covers an area of about 10 km^2 (Altunel & Hancock 1993*a*,*b*), located in the northeastern margin of the Denizli Basin (Westaway 1990, 1993, 1994; Alçiçek *et al.* 2007), in the Western Anatolian Extensional Province (Bozkurt 2001, 2003; Fig. 2), one of the most seismically active regions in the world (Eyidoğan 1988; Ambraseys & Finkel 1995; Bozkurt 2001). Extension in western Anatolia was active from late Oligocene time and gave rise to extensional detachments that promoted exhumation of HP–LT metamorphic rocks (Menderes Massif). The extensional detachments were later dissected by Neogene–Quaternary, SW–NE- and NW–SE-trending, high-angle normal faults, which define a basin and range structure (e.g. Şengör 1987; Yılmaz *et al.* 2000; Bozkurt 2001; Bozkurt & Oberhänsli 2001; Rimmelé *et al.* 2003, 2006; Alçiçek & ten Veen 2008; ten Veen *et al.* 2009; van Hinsbergen 2010). The basins are at present bounded by normal faults, many of them still active.

The Denizli Basin is a WNW–ESE-oriented structural depression, *c*. 70 km long and 50 km wide (Fig. 2), filled with a Neogene–Quaternary continental succession deposited in alluvial and lacustrine environments (Alçiçek *et al.* 2007). Recent (13 June 1965, 19 August 1976, 21 April 2000) and historical (1703, 1717) earthquakes indicate that the fault systems delimiting the southwestern and northeastern sides of the Denizli Basin have a high potential seismicity (Hancer 2013) with Magnitude 6 being recorded (Koçyiğit 2005).

Mesozoic successions stacked in a complex tectonic pile (Lycian Nappes) overlying a Palaeozoic–Mesozoic metamorphic succession referred to as the Menderes Massif (Collins & Robertson 1997; Rimmelé *et al.* 2003) are exposed in the northeastern margin of the basin, where Pamukkale is located (Fig. 2). A SW-dipping normal fault system mainly consisting of two fault segments (the Hierapolis and Akkoy segments; Altunel & Hancock 1993*a*) separates the Palaeozoic and Mesozoic successions from the Neogene and Quaternary continental sediments filling the basin (Şaroğlu *et al.* 1987, 1992; Çakir 1999; Hancock *et al.* 1999; Koçyiğit 2005), and plays a fundamental role in the hydrothermal circulation and fluid upwelling. The Pamukkale travertine plateau, where the ancient Hierapolis was built, is bounded by two SW-dipping faults. The southern one (the Akkoy fault) corresponds to the scarp on which travertine accumulated, giving rise to the spectacular Pamukkale range-front travertine slope. Kinematic data on the fault segments indicate a normal dip slip combined with a minor sinistral strike slip (Altunel & Hancock 1993*a*; Çakir 1999). Offsetting of Roman artefacts along the Hierapolis segment provides further evidence of fault activity in the Pamukkale area (Altunel & Hancock 1996). The NW–SE-trending faults delimiting the northeastern margin of the Denizli Basin are interrupted by two main NE–SW-trending faults that cross the whole Denizli Basin, resulting in segmented subparallel sub-basins, named the Laodikia and Çürüksu Grabens (see figs 2 and 6 of Kaymakci 2006). In particular, the northern NE–SW-trending fault interrupts the northern prolongation of the NW–SE-trending fault segments in the Akkoy area (Fig. 2c). Kinematic data on the NW–SE-trending faults indicate dominant normal movements, whereas a more articulated kinematics characterizes the NE–SW-trending faults, on which right- and left-lateral oblique slip as well as normal movements have been documented (Kaymakci 2006).

The carbonates making up the Pamukkale travertine body have been deposited since 400 ka and still are being deposited (Altunel & Hancock 1993*a*, *b*) by thermal waters with temperatures ranging from 35 to 56 °C (Şimşek *et al.* 2000; Kele *et al.* 2011; Özkul *et al.* 2013), rising from a carbonate bedrock (marble and calcschist) with permeability enhanced by the activity of extensional faults. The travertine deposits were studied by Altunel & Hancock (1993*a*,*b*, 1996), who described numerous morphologies and related depositional structures forming several fissure-ridges (Fig. 2). Among these structures, the Çukurbağ fissure-ridge has been studied mainly

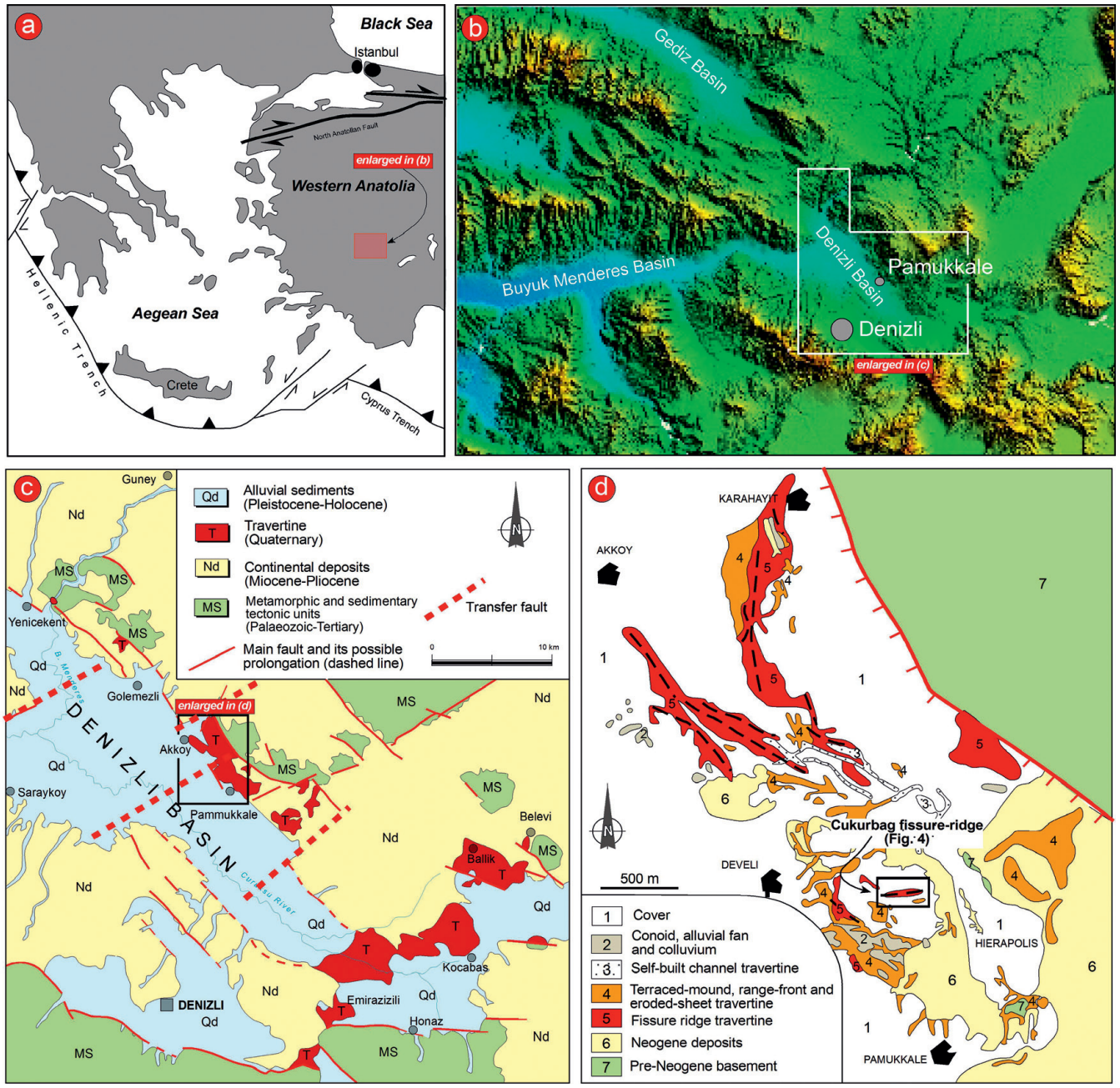

Fig. 2. Location of the study area: (**a**) western Anatolia and the Aegean Sea; (**b**) digital elevation model of the area including the Denizli Basin, where Pamukkale is located; (**c**) geological sketch map of the Denizli Basin and surroundings (from Sun 1990); (**d**) geological map of the Pamukkale area (from Altunel & Hancock 1993*a*).

from a morphotectonic perspective (Altunel & Hancock 1993*a*,*b*, 1996; Altunel & Karabacak 2005). Uysal *et al.* (2007) provided geochemical and U/Th radiometric data for some banded calcite veins in the Denizli Basin area and documented ages ranging from 151.19±0.8 to 24.9±0.1 ka. In particular, ages ranging from 25.2±0.2 to 24.9±0.1 ka were obtained for two banded and related bedded travertines from the Çukurbağ fissure-ridge by Uysal *et al.* (2009). Similar dates have been reported by De Filippis *et al.* (2012). Other radiometric data in the range of 29.5±1.4 and 21.5±1.0 ka were provided by Altunel & Karabacak (2005); these ages referred to dilation rates of about 0.10±0.02 and 0.07±0.003 mm a^{-1} during and after travertine deposition, respectively.

The Çukurbağ fissure-ridge

To obtain a better understanding of the geological processes controlling the growth of a fissure-ridge travertine deposit, the morphotectonic and depositional features of the Çukurbağ fissure-ridge are described.

Morphological setting

The Çukurbağ fissure-ridge is an uninterrupted morphotectonic feature, about 360 m long and 30 m wide, with a maximum height of 10 m (Fig. 3), which is characterized by a double change in

Fig. 3. (**a**) Panoramic view of the Çukurbağ fissure-ridge and the quarried area indicated by the anthropic build-up; (**b**) detail of the quarried area; (**c**, **d**) traces of the main work on the northern wall of the ridge; (**e**) a Roman column made of banded travertine abandoned at the margin of the quarried area.

orientation along its roughly east–west main direction so that it resembles a stretched S-shape. It strikes N110° in the western part for about 40 m, N75° in the central part for about 260 m and N90° in the eastern part for about 60 m (Fig. 4).

The ridge slopes have various inclinations (from 60° to less than 20°; Fig. 3) with the higher portion dipping away gently from the crest. On the whole, the ridge has an asymmetrical profile, with the northern slope steeper and locally higher than the southern one. The floor representing the substrate on which the travertine was deposited is characterized by higher elevation in the northern wall of the ridge, thus defining a morphological step hidden by the carbonate deposits (Fig. 5). The flanks of the ridge consist of several depositional units made of well-bedded or laminated travertine (bedded travertine); their inclined slopes include records of the original depositional morphologies (smooth and/or microterraced slope) resulting from the flow of the alkaline hot waters from the apical fissure.

The central part of the ridge corresponds to its highest elevation and width (Figs 4 and 5); therefore this sector was intensively quarried for building stone in Roman times. Ancient quarrying cuts reveal the internal structure of the fissure-ridge, showing a geometrically complex network of at least five (possibly up to eight) subparallel vein sets made of crystalline calcite and/or aragonite (banded travertine). Several almost parallel en-echelon and/or anastomosed fissures occur at the top of the ridge, along its crest. These fissures have a maximum opening of 170 cm and a maximum length of about 260 m. The fissure width decreases towards the tips, where it becomes about 1 mm.

Ridge lithofacies

Two main lithofacies (bedded and banded travertine) have been defined for the thermal carbonates on the basis of their composition, fabric and genesis (Altunel & Hancock 1993*a*,*b*). The bedded travertine comprises the subhorizontal to very steep, well-bedded and laminated lithofacies deposited in epigean conditions by the thermal waters flowing from the vent(s) along the lateral slopes (Fig. 6a). On the other hand, the term banded travertine relates to crystalline, laminated crusts precipitated in hypogean conditions as the infilling of vertical to subvertical fractures representing the conduits for the upwelling of thermal waters through the bedrock. Both facies are laterally related as they are deposited by the same water discharge during its flow from the internal circuit (where banded travertine precipitates in veins) to the external surface (where the bedded travertine is deposited in layered crusts) (Fig. 6b and c).

Geochemical variations and hydrodynamic behaviour of the thermal fluids, bacteria activity, and morphological roughness along the slope result in different depositional facies and facies associations (Guo & Riding 1998; Gandin & Capezzuoli 2008) and in rapid lateral facies changes, characteristic of the thermal depositional system (Guo & Riding 1998, 1999).

Bedded travertine. This consists of laminated layers (up to 2 m thick) of heterogeneous limestone of variable lateral extent, dipping from subhorizontal to subvertical (Fig. 6d) and pinching out from the central portion of the structure. The beds are composed of irregularly alternating laminae or bands (of centimetre to decimetre

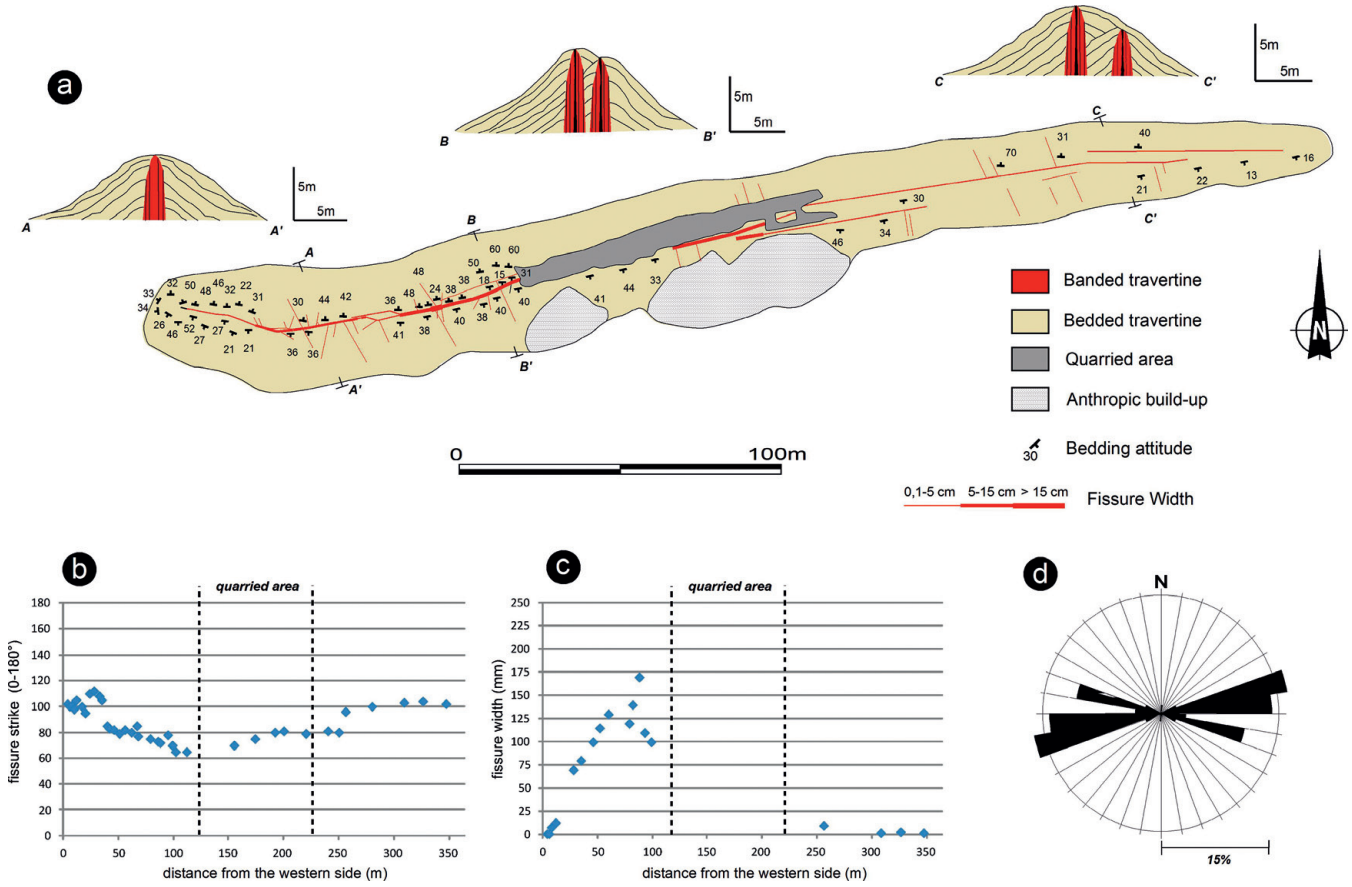

Fig. 4. (**a**) Schematic illustration of the morphotectonic features of the Çukurbağ fissure-ridge; (**b**) strike of the main fissure at the top of the ridge measured in the indicated position along the fissure-ridge; (**c**) fissure width v. position along the fissure-ridge; (**d**) rose diagram of the main fissure strike, located at the top of the ridge.

Fig. 5. Panoramic view of the Çukurbağ fissure-ridge (from the Hierapolis ruins) highlighting the morphological step on which the fissure-ridge developed: the southern floor is clearly located at a lower elevation with respect to the northern one.

size) of crystalline and microbial facies. Crystalline crusts are formed by superimposed or juxtaposed rows of feather-like crystals (Fig. 6e) or subordinately of very finely laminated fibrous fan-rays (Fig. 6f). These characteristic fabrics (Chafetz & Folk 1984) are indicative of high-energy flows on steep slopes (Capezzuoli & Gandin 2005; Gandin & Capezzuoli 2008). The crystalline facies are mostly located in the central, higher portion of the ridge, where they show highly inclined bedding and a compact fabric. In the lower, smoother to subhorizontal parts of the ridge the lithofacies association shows a generally more gentle inclination and a dominantly porous fabric (Fig. 6g and h) formed by laminar microbialites composed of shrubs and rafts and associated with micritic

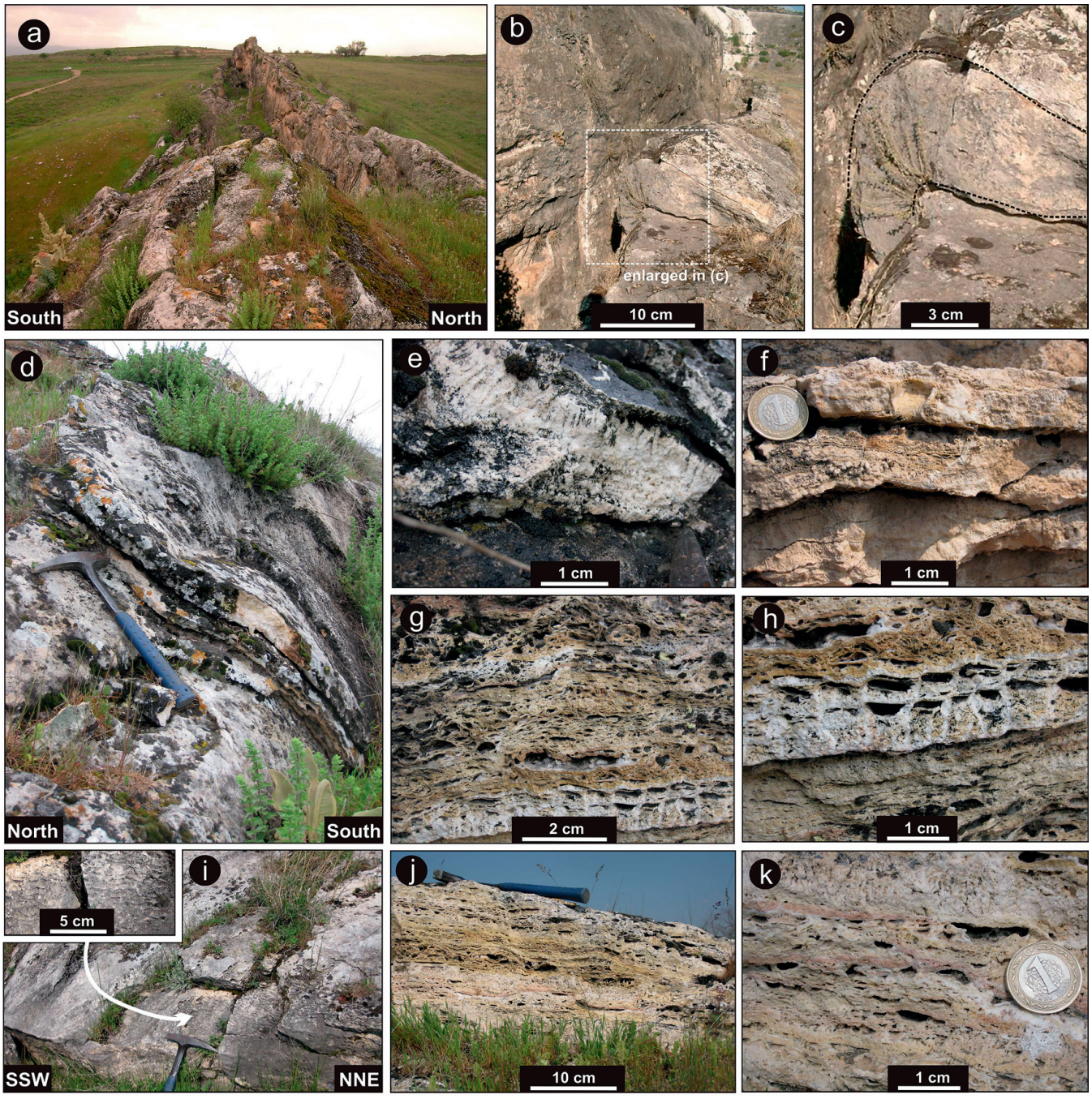

Fig. 6. (**a**) Highest part of the ridge showing the opposite dipping attitude of the travertine. (**b**, **c**) Key evidence highlighting the relation between the inclined–bedded travertine and the vertical, internal, banded travertine; this proves that banded and bedded travertines are genetically and physically linked and form from the same water rising along the central fissure and flowing on the external slope. (**d**) High-angle bedded travertine formed by crystalline crusts in the central part of the ridge. (**e**) Detail of the crust in (**d**) showing white feather crystals. (**f**) Example of fine-laminated crystalline crust. (**g**) Porous fabric of the bedded travertine in the apical portion. Bedding is more vague. (**h**) Detail of the lower part of (**g**) showing a vertical section of a low-angle microterraced slope. (**i**) Example of microterraced slope on the southern slope of the fissure-ridge. (**j**) Example of low-angle, gently undulated slope. (**k**) Alternation of fine laminated, porous travertine (lower portion) and compact, feather calcite crystalline crusts (upper portion).

laminae and lithoclasts (Fig. 6i and j). They are interpreted as the distal portion of the system, characterized by slow flow on microterraced or gently undulating low-angle slopes (Capezzuoli & Gandin 2005; Gandin & Capezzuoli 2008; Fig. 6k). The rapid lateral juxtaposition or shifting of all these depositional facies provides evidence of different microenvironments (waterfalls, pools, microterraced slopes, fans and smooth slopes) repeatedly following one upon the other, resulting from different episodes of deposition and diversion along the ridge, as also indicated by the numerous angular unconformities that bound the single depositional units.

Fig. 7. (**a**) Example of banded travertine with lithon of bedded travertine embedded; (**b**) detail of (**a**) highlighting the syntaxial calcite vein corresponding to a banded travertine vein; (**c**) internal part of the ridge widened for quarrying; (**d**) geometric relationships between banded and bedded travertine as recognizable in the internal part of the ridge; (**e**, **f**) micro-laminae typifying the fabric of the calcite veins (banded travertine); different colours indicate depositional episodes characterized by different fluid chemical compositions; (**g**–**i**) linkage between banded and bedded travertine; (**j**) cross-cutting relation between two veins defining a V-shaped pinching vertical banded crust isolating a lithon made of bedded travertine where the original fabric can be recognized.

Alternation of compact crystalline crusts and porous micritic laminae is very common and suggests fluctuation in water regime.

Banded travertine. This is formed by onyx-like, vertically banded white to brown calcite veins of centimetre to metre thickness cutting across the substrate and propagating to the surface (Fig. 7g–i) through the bedded travertine (Fig. 7a and b). Contacts between the banded travertine and the host rocks are usually sharp (Fig. 7b and d) and are locally characterized by embayed margins owing to replacement of the host rock. The vein thickness varies along the ridge: values are at a maximum (about 3 m) in the central and quarried portion of the ridge (Fig. 7c and d) and tend to decrease toward the ridge tips.

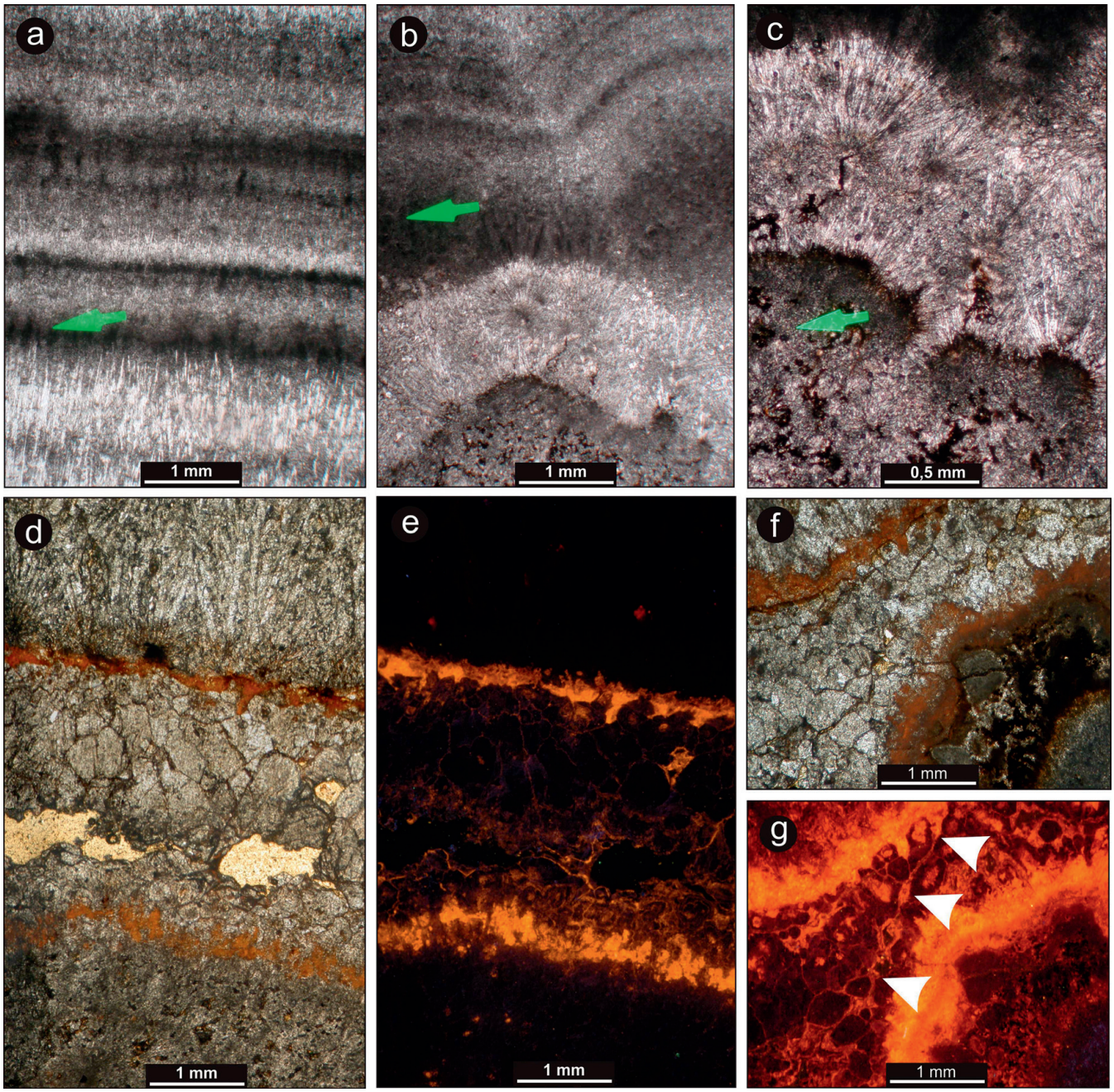

Fig. 8. (**a**) Multiple, superimposed laminae of banded travertine mainly formed by a dense palisade of acicular, needle-like crystals with pointed termination. (**b**) Example of ray-shaped fans of acicular crystals. (**c**) Micron-size, black alteration at the top of a lamina. The successive growth of a new crystal palisade from the alteration nucleus should be noted. (**d**) Alternation of acicular and blocky crystal laminae limited by levels of alteration. The 'ghost' acicular morphologies inside the blocky crystals should be noted. (**e**) CL image of same alternation of laminae as in (**d**). The banding testifies to different origins of the waters. It should be noted that blocky and acicular crystals have the same colours. (**f**) Banded laminae with acicular and blocky morphologies and alteration levels. (**g**) CL image of area shown in (**f**). Arrowheads indicate the continuity between the alteration level and rims of blocky crystals.

The banded travertine corresponds to vertical to subvertical laminated crusts or veins made of juxtaposed parallel or subparallel, millimetre to centimetre thick rows of palisade, fibrous or prismatic crystals grown in syntaxial continuity. The millimetre-scale zoning of the carbonate crystals is indicated by the irregular alternation of colourless and coloured (mainly rusty red or brown) crystal rows (Fig. 7e and f) depending on the mineral impurities (Fe- and/or Mn-oxides) included within the crystal lattices. The crystals or bands growing inward from the wall surfaces generally meet at the centre of the original open fissure or fracture, sealing it. The mid-line of the veins is locally marked by karstified voids of variable sizes (Fig. 7b). The trend of the vertical fractures is generally linear and is locally sinuous (Fig. 7b), probably because of wall anisotropy of the host rock. Pinched banded veins showing a V-shaped morphology (Fig. 7j) derived from superimposed veins that changed their trajectories during fissure evolution, and isolated lithons of previously deposited bedded travertine.

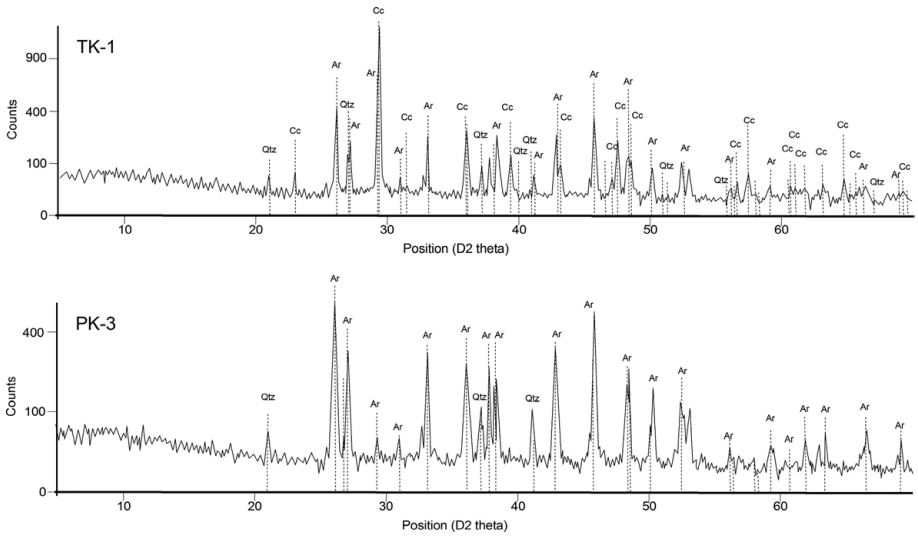

Fig. 9. X-ray diffraction (XRD) diagrams of two banded travertine samples collected from Vein A (see Fig. 10 for more details).

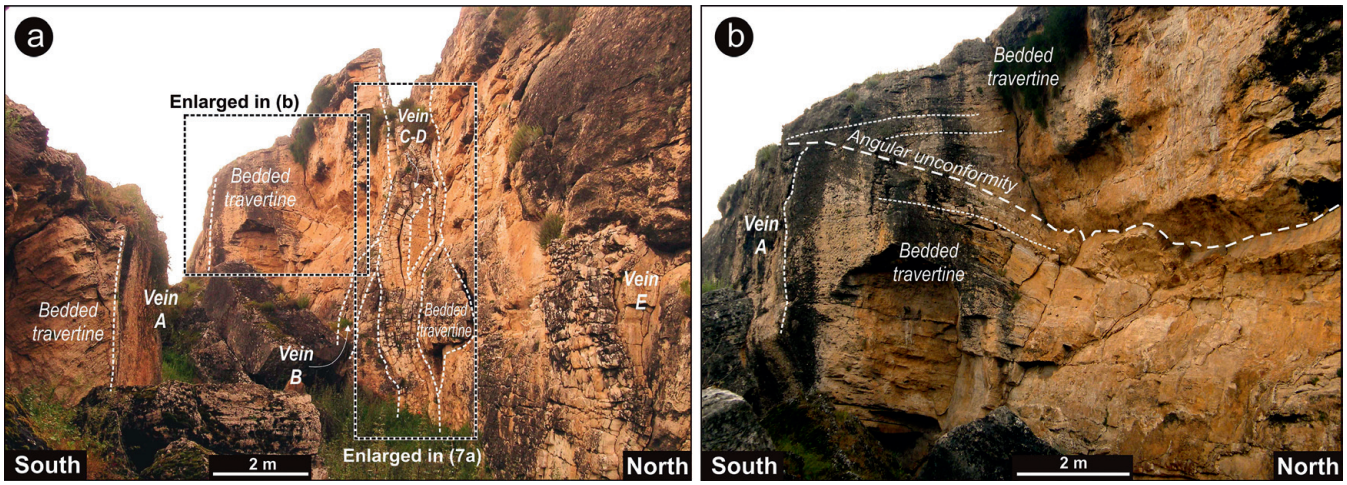

Fig. 10. (**a**) Banded–bedded travertine relation as recognizable in the internal part of the ridge. At least five generations of banded travertine veins can be recognized (veins A–E), indicating their progressive migration toward the northern wall; (**b**) opposite bedded travertine dipping attitude separated by an angular unconformity and testifying to the progressive rejuvenation toward the north of the banded–bedded system.

Detailed petrographic, cathodoluminescence (CL) and X-ray diffraction (XRD) analyses of the banded veins indicate how the elementary laminae are mainly formed by elongated crystals, mostly acicular (Fig. 8a) or prismatic, but also blocky in shape, growing normal to the walls of the fissures, forming dense assemblages devoid of primary porosity.

Most of the laminae are made of needle-like crystals of aragonite arranged in tight palisades with straight extinction or clusters of ray-shaped fans (Fig. 8b) similar to those described by Folk *et al.* (1985) and by Atabey (2002) for analogous lithofacies. Less frequently, laminae made of columnar–prismatic calcite and of blocky calcite (Fig. 8d–f) are present. The latter form exhibits a hypidiotopic, poikilotopic inequigranular fabric and growth competition textures (Friedman 1965) suggesting recrystallization at the expense of previous acicular aragonite that can be still be observed as ghosts inside the new blocky calcite crystals. Although most of the aragonite–calcite rows are in syntaxial continuity, randomly recurrent discontinuities between sets of laminae are marked by thin micron-size concentrations of opaque brown to black material (Fig. 8c and d) in a film corresponding to the meeting line of blocky crystals (Fig. 8e–g). This feature suggests temporary interruptions of the growth of the primary crystals, dissolution of aragonite–calcite, accumulation of residual material (Fe- and Mn-oxides) probably with the concurrence of microbial activity, and recrystallization–precipitation of blocky calcite. Such an interpretation is supported by the CL observations, which show a lack of luminescence of the elongated aragonite and calcite crystals or laminae (Fig. 8e–g) whereas bright, red-to-orange luminescence coincides with the films of opaque concentrations. The dissimilar luminescence behaviour is evidently related to the lack or presence of Mn within the calcite lattice and hence in the composition of the parent waters, and records a common derivation of the elongated crystals from Mn-free parent waters, probably of marine imprint, whereas a meteoric or soil-related Mn-rich parent water can be assumed to have originated the calcite films containing the residual material.

XRD analyses from Vein A show that the banded travertine mainly consists of pure aragonite with a minor component of quartz (sample PK-3, Fig. 9). Some laminae are formed by alternating aragonite and calcite bands (sample TK-1, Fig. 9), the latter composed of recrystallized blocky calcite crystals.

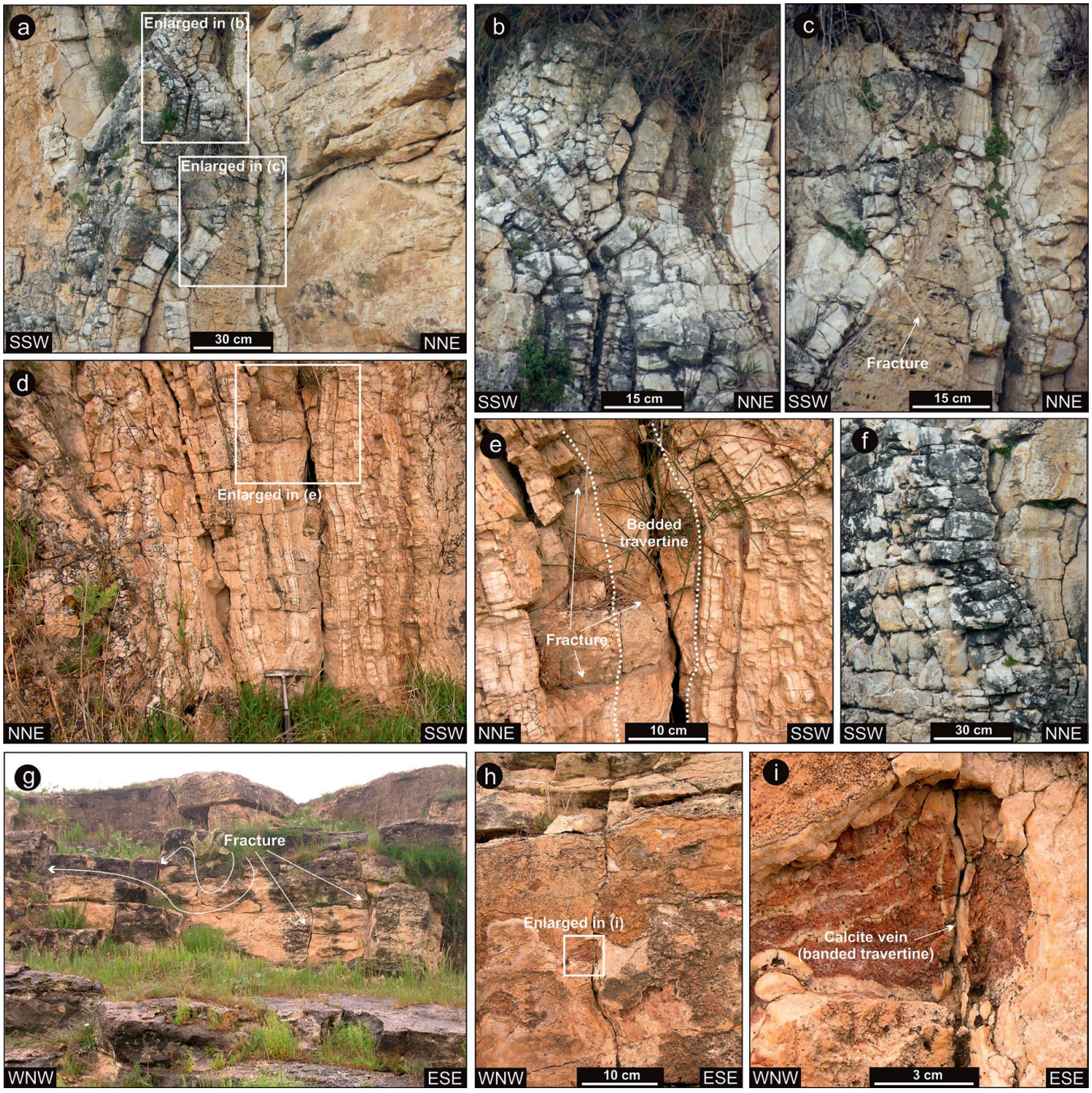

Fig. 11. Examples of banded veins showing brittle deformation. (**a-c**) Diffuse fractures affecting the different generations of banded travertine veins. In (**c**) it should be noted that the bedded travertine is fractured like the banded travertine. (**d**, **e**) Example of subhorizontal fractures affecting both banded and bedded travertine, in the inner part of the ridge. (**f**) Orthogonal intersecting fractures affecting the banded travertine in the inner part of the ridge. (**g**–**i**) Minor fractures affecting the bedded travertine and intersecting the main fissure at a high angle (see Fig. 4). These fractures are totally or partially filled by banded calcite veins like banded travertine, suggesting that fracturing occurred during fluid circulation.

Fissure-ridge internal anatomy and structural feature

The fresh cuts in the ancient quarry made it possible to investigate the internal part of the fissure-ridge, mainly in its central part (Fig. 4). At least five subparallel banded travertine veins run along the long axis of the ridge and are characterized by width ranging from 10 to 200 cm (Fig. 7). The crosscutting relationships between the banded travertine veins suggest their progressive northward migration. On the basis of their stratigraphic relationship, the oldest banded travertine vein (the widest one quarried by the Romans; Vein A in Fig. 10) crosses the ridge in its southernmost part. In contrast, the youngest banded travertine vein (Vein E in the Fig. 10) occupies the northernmost part of the ridge.

The banded travertine veins are intensely fractured in some parts (Fig. 11a and b), implying their brittle deformation. Fractures are not restricted to the banded travertine veins, but propagate also in the bedded travertine host rock (Fig. 11c–e), therefore suggesting a

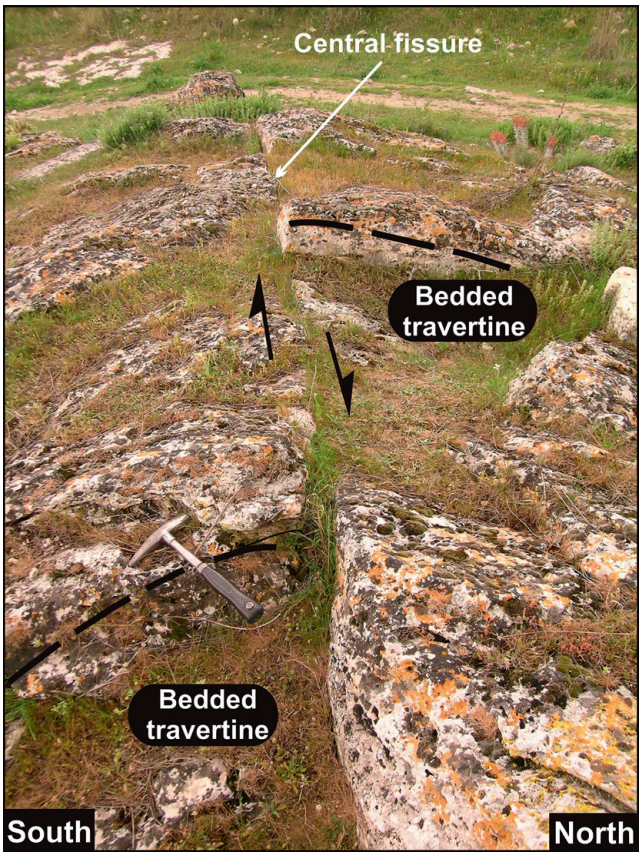

Fig. 12. Deca- to centimetre-sized offset occurring along the main fissure at the top of ridge in its western side, implying a right-lateral strike-slip movement during the development of the fissure-ridge.

deformational process that involved both fracture infill and bedded travertine host rock. Two main fracture sets have been recognized: (1) the most pervasive and widespread fracture set is characterized by roughly planar joints parallel to one another, relatively regularly spaced (from 1 cm to 10 cm); these joints cross the banded travertine veins at a high angle (Fig. 11a–e) defining subhorizontal intersection lines (Fig. 11f); (2) a fracture set, consisting of subvertical, NNW–SSE- and NNE–SSW-trending fractures that cross the banded travertine veins at a high angle and define subvertical intersection lines promoting the development of a network of orthogonal joints recognizable on the surface of the banded travertine veins (Fig. 11f). The subvertical joints also propagate in the northern and southern bedded travertine walls of the fissure-ridge and are mainly concentrated in the southern wall of the ridge (Fig. 11g). These joints are arranged both in en-echelon and in dihedral arrays (in plan view), and are concentrated in metre-wide domains having local high deformation density (i.e. the western side), characterized by 8–10 joints in 15 m (Fig. 4); in the other domains, density is lower and is 2–3 joints in 15 m on average. The angle between joints and the long axis of the ridge ranges from 60 to 80° (Fig. 4). Most joints have been filled by fibrous calcite crystals that grew in syntaxial mode, like the banded travertine veins (Fig. 11h and i), thus suggesting hydrothermal fluid circulation also in the peripheral fracture sets. In a few cases, banded veins are locally affected by sub-centimetre vertical offsets with a normal component of movement.

In the western part of the ridge, about 50 m from its margin, the fissure at the top of the ridge defines a rhomboid interrupted by two joints at low angle; such a feature resembles a step-over zone (Fig. 4) linking two fault-segments with right-lateral strike-slip movement. Indeed, the western side of the ridge, where the long axis trends N110° (see Fig. 4), is characterized by a right-lateral strike-slip offset of about 40 cm, displacing the northern wall from the southern wall of the ridge (Fig. 12). The slip surface corresponds to the main fissure at the top of the ridge. No kinematic indicators have been observed along the fault plane, but the transcurrent component can be inferred by the ridge-edge displacement (Fig. 12).

Discussion

The internal anatomy of the Çukurbağ fissure-ridge and its morphotectonic features (i.e. the crosscutting relationships between the various banded travertine veins, their progressive migration toward the northern wall of the fissure-ridge and the right-lateral offset along the main fissure at the top of the ridge) indicate that this body developed under the strict control of a fault zone active at least during the late Pleistocene–Holocene, as suggested by the radiometric age determination (Altunel & Karabacak 2005; Uysal *et al.* 2009; De Filippis *et al.* 2012). In addition, the relationships between banded and bedded travertine offer stimulating inputs to discuss the evolution of the fault zone that controlled the hydrothermal fluids up-flow and the conceptual mechanism for the development of the Çukurbağ fissure-ridge. In the following paragraphs first we discuss the role of the banded–bedded travertine in the tectonic interpretation; second, we focus on the possible mechanism that controlled the syntectonic growth of the Çukurbağ fissure-ridge with reference to an achievable mechanism driving the development of the whole fault-related travertine fissure-ridge. Finally, we discuss the west–east-trending Çukurbağ fault segment in the context of the NW–SE-trending active faulting that characterizes the northeastern side of the Denizli Basin in the Pamukkale area.

Banded–bedded travertine relation and its role in tectonic interpretation

The banded and bedded travertine lithofacies record the development of a syntectonic travertine body affected by brittle deformation (Figs 11 and 12); the fractures affecting the bedded travertine acted as conduits for hydrothermal fluids, which flowed at the surface and deposited new bedded travertine. Therefore the banded travertine veins represent a useful tool to understand the mechanism of the fissure-ridge development, as well as the relationships between tectonic activity and carbonate sedimentation in a geothermal system.

Banded travertine veins resemble calcareous sinter as defined by Koban & Schweigert (1993) owing to the well-developed lamination and lack of visible porosity (Flügel 2004). Pedley (1990) suggested that this term should be abandoned in favour of either tufa for ambient temperature deposits or travertine for geothermal carbonate deposits. The banded travertine consists of carbonate veins deposited by hydrothermal fluids and filling fractures affecting travertine masses. The micro-laminated fabric (Fig. 8), coupled with the syntaxial growth process (Fig. 7a and b), indicates that such veins were the consequence of the crack-and-seal process (see Sibson 1987), which is indicative of repeated fracture opening pulses followed by periods of carbonate deposition, often giving rise to aragonitic–calcitic laminae. The deposition of aragonite is favoured by rapid precipitation rate, high pCO_2, and elevated Mg/Ca (Pichler & Veizer 2004). Owing to the rapid precipitation rate, the banded travertine veins can minutely record deposition that occurred during short time spans and is represented

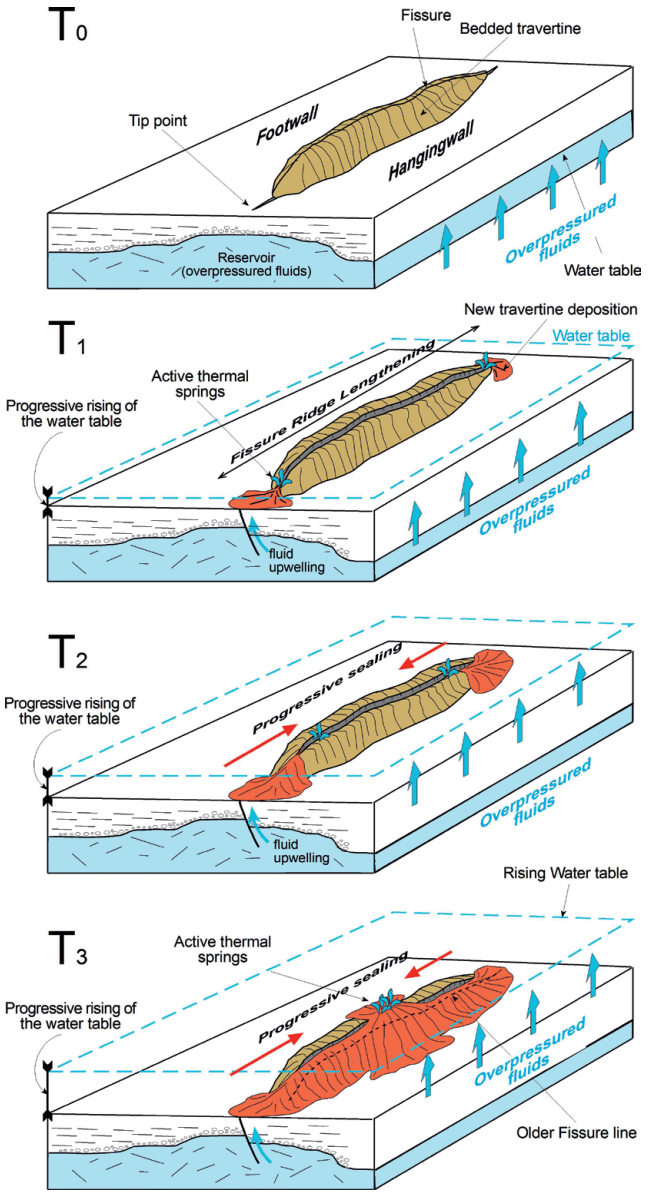

Fig. 13. Schematic illustration of the conceptual mechanism controlling the development of a travertine fissure-ridge. T_0 illustrates the fissure-ridge during a tectonically quiescent period; at that time, the permeability was totally destroyed as a result of fracture sealing by calcite veins (i.e. banded travertine). After a tectonic pulse the fault reactivates, reopening previously sealed fractures and allowing the overpressured fluids to rise (T_1). Fluids discharge at the tip zones; here flow is favoured by the hydraulic gradient. Progressive fluid flow seals the fractures at the ends of the ridge; consequently, the springs have to migrate toward the higher portions of the ridge (T_2) up to the highest part (T_3). At that time, fracture sealing progressively inhibits fluid flow and the travertine deposition stops. A subsequent period of travertine deposition and fluid flow can be guaranteed by a new tectonic pulse.

by thick crystalline layers. For example, radiometric dating of some banded travertine veins crossing the Çukurbağ fissure-ridge (Uysal *et al.* 2009) indicates that a banded travertine vein of about 40 cm thickness is representative of about 200 years.

The presence of biological alteration at the top of many laminae (Fig. 8c and d) suggests that fracture walls were periodically exposed to the air, and so the vein surface was altered by biological activity. This implies that, in some cases, vein opening was not accompanied by instantaneous water flow.

The intimate association of banded travertine veins with seismicity and their triggering of mobilization of CO_2-rich fluids have been extensively demonstrated (Altunel & Karabacak 2005; Uysal *et al.* 2009). In this sense, banded travertine vein networks most probably represent the best near-surface product of CO_2-driven hydrothermal eruptions in seismically active zones (Uysal *et al.* 2007, 2009). However, it is also perceived that they are important as a possible palaeoclimate recorder, considering that the CO_2-driven hydrothermal eruption process may be driven by global and regional climate, as has been more significantly recognized during dry climate periods in the late Quaternary (Uysal *et al.* 2009). Thus, although climate could represent another key factor promoting hydrothermal circulation (see Faccenna *et al.* 2008; De Filippis *et al.* 2013*a*), tectonic activity is fundamental to guarantee fracture opening and related permeability in the rock masses, which is indispensable to promoting the hydraulic connection of the reservoir with the surface. Accordingly, the travertine fissure-ridges, where banded and bedded travertine are intimately connected, are the most significant travertine masses for tectonic investigations.

Growth and development mechanism of a fault-controlled fissure-ridge

The growth and development mechanisms of the Çukurbağ fissure-ridge were strictly influenced by the fault zone evolution, which can be ascribed to repeated cycles for which two main coexisting factors were essential: (1) improvement of localized (fault-related) permeability in the bedrock; (2) occurrence of overpressured thermal, alkaline and CO_2-rich fluids channelled along the interconnected fracture system forming the fault damage zone. The interplay between tectonic activity, improved and destroyed permeability, fluid flow, fluid degassing and travertine deposition regulated the development of the fissure-ridge.

Altunel & Hancock (1993*a*, *b*, 1996) and Hancock *et al.* (1999) interpreted the Pamukkale travertine fissure-ridges as morphotectonic features developed in step-over zones along the main NW–SE-trending normal fault system bounding the northeastern shoulder of the Denizli Basin. Overall those researchers interpreted the NW–SE- and east–west-striking travertine fissure-ridges as travertine-filled dilatational fractures, related to the progressive opening of fractures in the bedrock (fracture is here used as a general term indicating a mode-I joint; Pollard & Aydin 1988) of the hanging wall of the Akkoy fault segment (Fig. 2). Although this is the general conclusion for most Altunel and Hancock's papers dealing with the travertine fissure-ridges at Pamukkale, they also reported the case of an unspecified fissure-ridge grown on a fault scarp, characterized by 'a downthrow of about 5 m along 250 m of its 500 m length' (Altunel & Hancock 1996), implying a strict relationship between the fissure-ridge and faulting. A contrasting hypothesis and a different interpretation were given for the Çukurbağ fissure-ridge, which was interpreted by Altunel & Hancock (1993*a*, *b*) and Hancock *et al.* (1999) as a dilatational fissure reflecting the local influence of the north–south extension direction that characterizes the Menderes graben.

An alternative conceptual model dealing with the development of a travertine fissure-ridge has been proposed by De Filippis *et al.* (2012), who described four growth phases giving rise to the complete fissure-ridge development. In phase 1, a fissure-ridge consisting of a linear elongated travertine mound grows on top of hot springs. As the fissure-ridge grows the accumulated travertine forming the ridge, together with the differential subsidence acting in a part of the ridge, increasingly hinders direct outflow from the

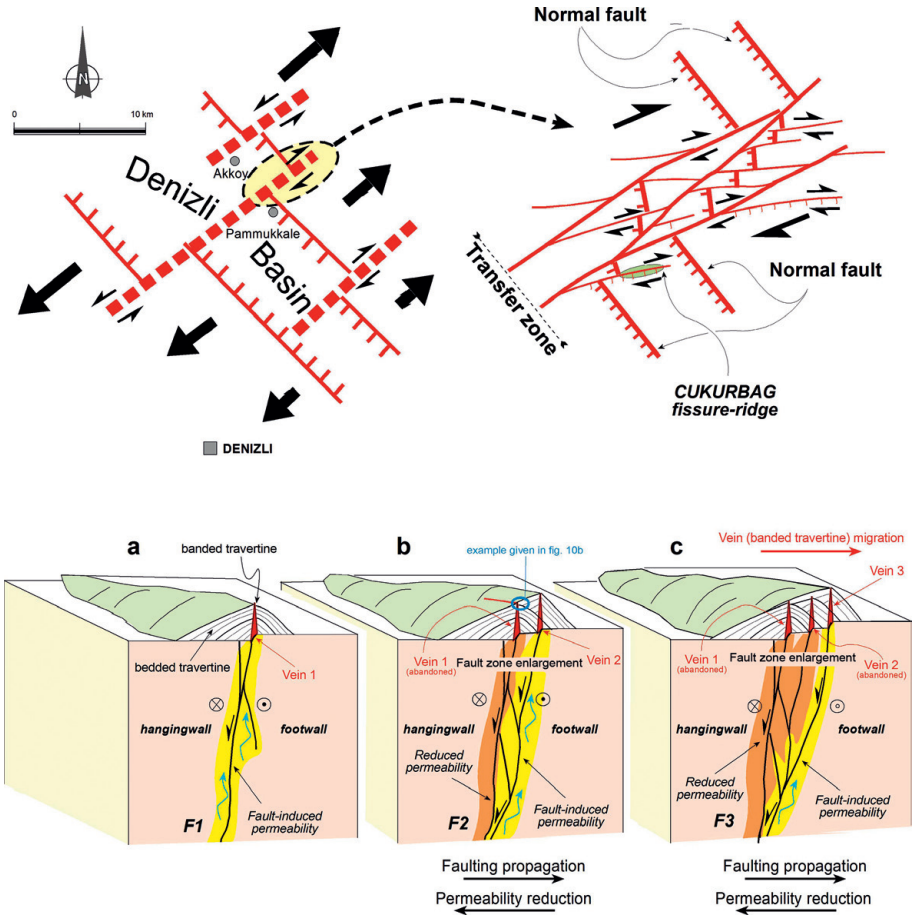

Fig. 14. Schematic illustrations: the (conceptual) tectonic model of the Denizli Basin; the relationships between the transfer zone and the Çukurbağ fissure-ridge, based on our field data and those by other researchers (Sun 1990; Altunel 1994; Altunel & Hancock 1996; Kaymakci 2006; Alçiçek *et al.* 2007); the fault zone evolution promoting the Çukurbağ fissure-ridge growth.

central feeding conduit (phase 2). At that point, an overpressure of the hydrothermal fluids develops, producing hydraulic fracturing followed by depressurization, which is the cause of the various generations of cross-cutting fissures filled by banded travertine (phases 3 and 4). De Filippis *et al.* (2012; see their fig. 11) considered the Çukurbağ fissure-ridge as a key element to describe the third growth phase. Although this evolution takes into consideration the main features of a fissure-ridge (i.e. superimposed banded travertine veins, V-shape of some banded travertine veins), some other evidence (i.e. the shape and geometry of the fissure-ridges, the different elevation of the walls, the migration of the banded travertine, the permeability increase or destruction) needs to be better understood. In our opinion, data collected in the Çukurbağ fissure-ridge allow us to focus on some important elements improving the conceptual model for fissure-ridge development.

The asymmetric profile of the fissure-ridge (Fig. 5) implies that the substratum does not consist of tabular bedrock, but it is characterized by a step of about 5 m in height, over which the travertine is draped. This definitively accounts for the fault step on which the ridge grew. Evidence based on the banded–bedded travertine relation is indicative of a syn-faulting travertine deposition. Figure 6b and c show the youngest banded travertine vein progressively passing to the bedded travertine laminated crust located at the top of the southern travertine wall, thus providing support for the deposition of the younger travertine across that side of the fissure-ridge. In the same way, Figure 7g and h clearly shows that the topmost part is lower than the bedded travertine forming the top of the northern half. This implies that the fissure separating the two halves of the ridge unequivocally runs along the trace of a fault. On the other hand, there is unambiguous evidence of brittle deformation affecting the banded and bedded travertine (Fig. 11) that supports the occurrence of deformation after travertine deposition, as also confirmed by the horizontal right-lateral strike-slip movement reconstructed in the western side of the ridge (Fig. 12). Similar data were also reported by Altunel (1994). Surely the present configuration of the fissure-ridge is the consequence of a multi-stage process characterized by repeated faulting pulses that promoted permeability, fluid flow, travertine deposition and then growth of the fissure-ridge. In our opinion, the differential subsidence acting in a part of the ridge, mentioned by De Filippis *et al.* (2012), can be referred to faulting. The different generations of cross-cutting banded veins ascribed by De Filippis *et al.* (2012) to combined gravitational and hydraulic effects, are the clear expression of a tectonic process. Thus the ridge fissuring, as well as the emplacement of the banded veins, was primarily driven by tectonics, although we cannot exclude temporary hydrothermal eruptions as a secondary effect.

Figure 13 shows the main steps for the development of a fault-related fissure-ridge after a single tectonic pulse, defining a fissure-ridge growth-cycle: tectonic activity gives rise to fault reactivation, which increases the permeability mainly at the tips of the fault segment, where new fractures can guarantee fault propagation (T_1 in Fig. 13). At that time, overpressured fluids trapped in the reservoir at depth are channelled along the new fractures, feeding thermal springs located at the extremities of the ridge, as these are the lowermost points available for resurgence owing to hydraulic pressure. Hydrothermal fluids leave the dissolved CO_2, triggering the precipitation of travertine that accumulates at ridge margins. The progressive travertine deposition tends to seal the

fractures and prevent a continuous fluid discharge. Nevertheless, permeability destruction at the ridge margins favours the rise of the water table, which will feed thermal springs located along the fissure and at higher elevation (T_2 in Fig. 13). Progressive travertine deposition and related permeability destruction provide the progressive thermal spring migration up to the top of the ridge, guaranteeing travertine deposition in the higher portion of the ridge (T_3 in Fig. 13).

The complete sealing of fractures feeding thermal springs inhibits travertine deposition and defines the end of the growth-cycle. The following tectonic pulse(s), coupled with availability of thermal water owing to favourable climatic conditions, can renew the permeability, offering the opportunity for repeated growth-cycles and giving rise to the progressive ridge development. In the case of a tectonic pulse during an arid period, new opened fractures are exposed to the air, therefore banded travertine is prone to alteration by microbial activity, and growth evolution of the ridge is interrupted.

The morphology and internal anatomy of the ridge are strictly influenced by the evolution of the fault zone. The example of the Çukurbağ fissure-ridge suggests that the relationships between the banded and bedded travertine can reveal much on this topic: the various generations (at least five) of banded travertine veins (and coeval bedded travertine) progressively migrate toward the northern half of the ridge. This can be deduced from the fact that bedded travertine dipping away from a central fissure was successively buried by bedded travertine dipping in the opposite direction (Fig. 10), which originated from fluids flowing from a new fissure that developed in the peripheral northern wall. Such a migration is strictly related to a fault zone evolution characterized by its progressive growth in the footwall. Figure 14 shows the possible conceptual evolution of the fault zone: the local stress field gave rise to a main fault plane with associated minor structures (Fig. 14a); successive variation in the dip-slip or in the strike-slip component, as usual in transfer zones (see the next section) could have favoured the occurrence of most damage in the footwall block, thus defining another main slip plane (Fig. 14b). Successive tectonic pulses could have enlarged the fault zone, defining a progressive growth in the footwall zone (Fig. 14c).

Regional consideration

The west–east-striking fault zone of the Çukurbağ fissure-ridge was active contemporaneously with the main NW–SE-striking normal fault segments delimiting the northeastern side of the Denizli Basin and producing the SW-dipping slope on which the Pamukkale travertine was deposited (Altunel 1994; Fig. 2). All faults acted as conduits for hydrothermal circulation, implying their hydraulic connection at depth. De Filippis *et al.* (2012) presented a conceptual model for the fissure-ridges at Pamukkale, explaining the hydrothermal system as driven by a NW–SE-trending relatively low-angle normal fault system and associated parallel fractures affecting the hanging wall and feeding the fluids (see fig. 11 of De Filippis *et al.* 2012). If their model is used to explain the fissure-ridges in the Pamukkale area, then the near-orthogonal orientation of the Cukurbag fissure-ridge with respect to the master fault system has to be explained.

The right-lateral component in the western side of the ridge suggests that the Çukurbağ fissure-ridge developed on a fault zone with a lateral component, although the morphological step and the down-dip movement of the southern wall of the fissure-ridge also suggest a dominant normal component (Fig. 5). Consequently, although the complete kinematic history of the fault zone cannot be defined, we can speculate that the Çukurbağ fault zone was the result of the interplay between strike-slip and normal faulting, resulting in a right-lateral transtensional kinematics with a dominant normal offset (at least 5 m) and a minor right-lateral one (about 40 cm). The right-lateral movement contrasts with the shape of the ridge (in plan view), implying that the long tract of the ridge acted as a restraining band, thus contrasting with the main fissure dilatation in the central part. On the other hand, the lateral offset (40 cm) is surely irrelevant and took place in a general context dominated by normal movements.

The coexistence of a west–east-striking right-lateral transtensional fault and NE–SW-trending normal faults has to be explained. We suggest that the Çukurbağ fault belongs to a transfer fault system (i.e. an accommodation zone) interfering with the master fault system delimiting the basin. In fact, normal and strike-slip kinematics for orthogonal fault systems can coexist in extensional fault systems, characterized by normal faults defining a graben and/or half-graben, transferred by accommodation shear zones composed of fault segments often characterized by strike-slip to oblique-slip movements (Gibbs 1984, 1990). Kinematic information on the main and minor faults of the Denizli Basin highlights NW–SE-trending faults with dominant normal movements, and NE–SW-trending faults showing right-lateral and left-lateral oblique-slip and normal kinematics, often recognizable on the same fault plane (Kaymakci 2006). Similar superimposed kinematic indicators on faults, acting as transfer zones and accompanying the development of Quaternary basins in the surroundings of the Denizli Basin, have been described by Alçiçek *et al.* (2013).

The NW–SE-trending fault system in the Pamukkale area is intersected by a regional NE–SW-striking fault system (Fig. 2c) showing latest Pleistocene strike-slip kinematics (van Noten *et al.* 2013) and defining a corner where thermal springs and travertine deposition were and are concentrated (Fig. 2c).

On the other hand, it has been also documented that accommodation zones are the most efficient structural environment guaranteeing hydrothermal circulation in geothermal systems (Rowland & Sibson 2004), as intersecting orthogonal fault segments can give rise to very highly damaged rock masses (Curewitz & Karson 1997; Brogi 2004; Brogi *et al.* 2012). A similar explanation has been given for the tectonically controlled fissure-ridges at Cambazli (located 130 km NW of Pamukkale), which have been considered to be controlled by a shear zone acting as a transfer zone accommodating the development of the normal faults delimiting the Gediz Graben (Temiz & Eikenberg 2011).

Concluding remarks

The Çukurbağ travertine fissure-ridge is a tectonically controlled travertine body that developed on a fault zone of at least 360 m length, with a possible transtensional kinematics, active during the late Pleistocene–Holocene. Such a fault is possibly a minor structure belonging to a more important NE–SW-trending fault system that acted as a transfer zone accommodating the NW–SE-trending normal fault system delimiting the NE margin of the Denizli Graben (Fig. 14).

The banded–bedded travertine relation as well as the cross-cutting relationships between the banded travertine veins represent the main tool to infer the development mechanism for the fissure-ridge growth, and to obtain information on the regional tectonics affecting the area. For this purpose, our main results for the Çukurbağ fissure-ridge are as follows (Fig. 14).

(1) It is a syntectonic travertine body.

(2) Its morphotectonic features developed under the strict control of a fault zone, which became enlarged during its progressive development.

(3) Brittle deformation associated with faulting propagated within the bedded travertine mainly belonging to the northern half of the ridge, resulting in at least five banded travertine veins; these veins were not synchronous and migrated through time, indicating that deformation progressively affected the footwall, contemporaneously with the downward displacement of the southern half (Fig. 14).

In a more general view, the main results for the travertine fissure-ridges are as follows. The complete development of a fault-controlled travertine fissure-ridge can be considered as related to multiple growth-cycles controlled by fault activity. Each tectonic pulse produces progressive enlargement and lengthening of the fault segment, enhancing the permeability at the tip zones and allowing fluid flow owing to fluid overpressure; fluid discharge deposits bedded travertine at the fault tips, progressively destroying the permeability owing to rapid fracture sealing. Fluid overpressure leads to a rise of the table water and related activation of springs in the highest portions of the ridge, until the progressive sealing of the fissure, which guarantees the banded travertine growth (Fig. 13).

In sum, the banded–bedded travertine relation represents a useful tool to reconstruct the palaeotectonic activity in a region.

We are grateful to E. Altunel and E. Bozkurt for the criticisms and constructive comments that allowed us to improve the original version of the paper. M.C.A. received the grant of Outstanding Scientist Award by the Turkish Academy of Sciences.

References

Alçiçek, H., Varol, B. & Özkul, M. 2007. Sedimentary facies, depositional environments and palaeogeographic evolution of the Neogene Denizli Basin of SW Anatolia, Turkey. *Sedimentary Geology*, **202**, 596–637, http://dx.doi.org/10.1016/j.sedgeo.2007.06.002.

Alçiçek, M.C. & ten Veen, J.H. 2008. The late Early Miocene Acıpayam piggyback basin: Refining the last stages of Lycian Nappes emplacement in SW Turkey. *Sedimentary Geology*, **208**, 101–113, http://dx.doi.org/10.1016/j.sedgeo.2008.05.003.

Alçiçek, M.C., Brogi, A., Capezzuoli, E., Liotta, D. & Meccheri, M. 2013. Superimposed basins formation during the Neogene–Quaternary extensional tectonics in SW Anatolia (Turkey): Insights from the kinematics of the Dinar Fault Zone. *Tectonophysics*, **608**, 713–727, http://dx.doi.org/10.1016/j.tecto.2013.08.008.

Altunel, E. 1994. *Active tectonics and the evolution of Quaternary travertines at Pamukkale, Western Turkey*. PhD thesis, University of Bristol.

Altunel, E. & Hancock, P.L. 1993*a*. Active fissuring and faulting in Quaternary travertines at Pamukkale, Western Turkey. *Zeitschrift für Geomorphologie Supplement*, **94**, 285–302.

Altunel, E. & Hancock, P.L. 1993*b*. Morphology and structural setting of Quaternary travertines at Pamukkale, Turkey. *Geological Journal*, **28**, 335–346.

Altunel, E. & Hancock, P.L. 1996. Structural attributes of travertine-filled extensional fissures in the Pamukkale Plateau, Western Turkey. *International Geology Review*, **38**, 768–777.

Altunel, E. & Karabacak, V. 2005. Determination of horizontal extension from fissure-ridge travertines: A case study from the Denizli Basin, southwestern Turkey. *Geodinamica Acta*, **18**, 333–342, http://dx.doi.org/10.3166/ga.18.333-342.

Ambraseys, N.N. & Finkel, C. 1995. *The Seismicity of Turkey and Adjacent Areas. A Historical Review 1500–1800*. Eren Yayıncılık, Istanbul.

Atabey, E. 2002. The formation of fissure ridge type laminated travertine–tufa deposits microscopical characteristics and diagenesis, Kirşehir, Central Anatolia. *Bulletin of the General Directorate of Mineral Research and Exploration of Turkey*, **123–124**, 59–65.

Aydin, A. 2000. Fractures, faults and hydrocarbon entrapment, migration, and flow. *Marine and Petroleum Geology*, **17**, 797–814, http://dx.doi.org/10.1016/S0264-8172(00)00020-9.

Bargar, K.E. 1978. Geology and thermal history of Mammoth Hot springs, Yellowstone National Park, Wyoming. *US Geological Survey Bulletin*, **1444**, 1–55.

Becken, M. & Ritter, O. 2012. Magnetotelluric studies at the San Andreas Fault Zone: Implications for the role of fluids. *Surveys in Geophysics*, **33**, 65–105, http://dx.doi.org/10.1007/s10712-011-9144-0.

Becken, M., Ritter, O., Bedrosian, P.A. & Weckmann, U. 2011. Correlation between deep fluids, tremor and creep along the central San Andreas Fault. *Nature*, **480**, 87–90, http://dx.doi.org/10.1038/nature10609.

Bellani, S., Brogi, A., Lazzarotto, A., Liotta, D. & Ranalli, G. 2004. Heat flow, deep temperatures and extensional structures in the Larderello geothermal field (Italy): Constraints on geothermal fluid flow. *Journal of Volcanology and Geothermal Research*, **132**, 15–29, http://dx.doi.org/10.1016/S0377-0273(03)00418-9.

Bozkurt, E. 2001. Late Alpine evolution of the central Menderes Massif, western Turkey. *International Journal of Earth Sciences*, **89**, 728–744, http://dx.doi.org/10.1007/s005310000141.

Bozkurt, E. 2003. Origin of NE-trending basins in western Turkey. *Geodinamica Acta*, **16**, 61–81, http://dx.doi.org/10.1016/S0985-3111(03)00002-0.

Bozkurt, E. & Oberhänsli, R. 2001. Menderes Massif (Western Turkey): Structural, metamorphic and magmatic evolution—a synthesis. *International Journal of Earth Sciences*, **89**, 679–708, http://dx.doi.org/10.1007/s005310000173.

Brogi, A. 2004. Faults linkage, damage rocks and hydrothermal fluid circulation: Tectonic interpretation of the Rapolano Terme travertines (southern Tuscany, Italy) in the context of the Northern Apennines Neogene–Quaternary extension. *Eclogae Geologicae Helvetiae*, **97**, 307–320, http://dx.doi.org/10.1007/s00015-004-1134-5.

Brogi, A. & Capezzuoli, E. 2009. Travertine deposition and faulting: The fault-related travertine fissure-ridge at Terme S. Giovanni, Rapolano Terme (Italy). *Geologische Rundschau*, **98**, 931–947, http://dx.doi.org/10.1007/s00531-007-0290-z.

Brogi, A., Capezzuoli, E., Buracchi, E. & Branca, M. 2012. Tectonic control on travertine and calcareous tufa deposition in a low-temperature geothermal system (Sarteano, Central Italy). *Journal of the Geological Society, London*, **169**, 461–476, http://dx.doi.org/10.1144/0016-76492011-137.

Caine, S.J., Evans, J.P. & Forster, C.B. 1996. Fault zone architecture and permeability structure. *Geology*, **24**, 1025–1028, http://dx.doi.org/10.1130/0091-7613(1996)024<1025:FZAAPS>2.3.CO;2.

Çakir, Z. 1999. Along-strike discontinuity of active normal faults and its influence on Quaternary travertine deposition: Examples from Western Turkey. *Turkish Journal of Earth Sciences*, **8**, 67–80.

Capezzuoli, E. & Gandin, A. 2005. Facies distribution and microfacies of thermal-spring travertine from Tuscany. *In*: Özkul, M., Yagiz, S. & Jones, B. (eds) *Proceedings of 1st International Symposium on Travertine, Pamukkale University, Denizli (Tr)*. Kozan Ofset, Ankara, 43–50.

Capezzuoli, E., Gandin, A. & Pedley, H.M. 2013. Decoding tufa and travertine (freshwater carbonates) in the sedimentary record: The state of the art. *Sedimentology*, http://dx.doi.org/10.1111/sed.12053.

Chafetz, H.S. & Folk, R.L. 1984. Travertines: Depositional morphology and the bacterially constructed constituents. *Journal of Sedimentary Petrology*, **54**, 289–316.

Collins, A.S. & Robertson, A.H.F. 1997. Lycian melange, southwestern Turkey: An emplaced Late Cretaceous accretionary complex. *Geology*, **25**, 255–258, http://dx.doi.org/10.1130/0091-7613(1997)025<0255:LMSTAE>2.3.CO;2.

Curewitz, D. & Karson, J.A. 1997. Structural settings of hydrothermal outflow: Fracture permeability maintained by fault propagation and interaction. *Journal of Volcanology and Geothermal Research*, **79**, 149–168, http://dx.doi.org/10.1016/S0377-0273(97)00027-9.

De Filippis, L. & Billi, A. 2012. Morphotectonics of fissure ridge travertines from geothermal areas of Mammoth Hot Springs (Wyoming) and Bridgeport (California). *Tectonophysics*, **548–549**, 34–38, http://dx.doi.org/10.1016/j.tecto.2012.04.017.

De Filippis, L., Faccenna, C., *et al.* 2012. Growth of fissure ridge travertines from geothermal springs of Denizli basin, western Turkey. *Geological Society of America Bulletin*, **124**, 1629–1645, http://dx.doi.org/10.1130/B30606.1.

De Filippis, L., Faccenna, C., Billi, A., Anzalone, E., Brilli, M., Soligo, M. & Tuccimei, P. 2013*a*. Plateau versus fissure ridge travertines from Quaternary geothermal springs of Italy and Turkey: Interactions and feedbacks between fluid discharge, paleoclimate, and tectonics. *Earth-Science Reviews*, **123**, 35–52.

De Filippis, L., Anzalone, E., Billi, A., Faccenna, C., Poncia, P.P. & Sella, P. 2013*b*. The origin and growth of a recently-active fissure ridge travertine over a seismic fault, Tivoli, Italy. *Geomorphology*, **195**, 13–26.

Eyidoğan, H. 1988. Rates of crustal deformation in western Turkey as deduced from major earthquakes. *Tectonophysics*, **148**, 83–92, http://dx.doi.org/10.1016/0040-1951(88)90162-X.

Faccenna, C., Funiciello, R., Montone, P., Parotto, M. & Voltaggio, M. 1993. Late Pleistocene strike slip tectonics in the Acque Albule basin (Tivoli, Latium). *Memorie Descrittive della Carta Geologica d'Italia*, **69**, 37–50.

Faccenna, C., Soligo, M., Billi, A., De Filippis, L., Funiciello, R., Rossetti, C. & Tuccimei, P. 2008. Late Pleistocene depositional cycles of the Lapis Tiburtinus travertine (Tivoli, central Italy): Possible influence of climate and fault activity. *Global and Planetary Change*, **63**, 299–308, http://dx.doi.org/10.1016/j.gloplacha.2008.06.006.

Flügel, E. 2004. *Microfacies of Carbonate Rocks: Analysis, Interpretation and Application*. Springer, Berlin.

Folk, R.L., Chafetz, S. & Tiezzi, P.A. 1985. Bizarre forms of the depositional and diagenetic calcite in hot-spring travertines, Central Italy. *In*: Schneidrmann, N. & Harris, P.M. (eds) *Carbonate Cements*. *Society of Economic Paleontologists and Mineralogists, Special Publications*, **36**, 349–369.

Ford, T.D. & Pedley, H.M. 1996. A review of tufa and travertine deposits of the world. *Earth-Science Review*, **41**, 17–175, http://dx.doi.org/10.1016/S0012-8252(96)00030-X.

Friedman, G.M. 1965. Terminology of recrystallization textures and fabrics in sedimentary rocks. *Journal of Sedimentary Petrology*, **35**, 643–655, http://dx.doi.org/10.1306/74D7131B-2B21-11D7-8648000102C1865D.

Gandin, A. & Capezzuoli, E. 2008. Travertine versus calcareous tufa: Distinctive petrologic features and stable isotopes signatures. *Italian Journal of Quaternary Science*, **21**, 125–136.

Gibbs, A.D. 1984. Structural evolution of extensional basin margins. *Journal of the Geological Society, London*, **141**, 609–620.

Gibbs, A.D. 1990. Linked faults in basin formation. *Journal of Structural Geololgy*, **12**, 795–803.

Gratier, J.P., Favreau, P., Renard, F. & Pili, E. 2002. Fluid pressure evolution during the earthquake cycle controlled by fluid flow and pressure solution crack sealing. *Earth Planets Space*, **54**, 1139–1146.

Guo, L. & Riding, R. 1998. Hot-spring travertine facies and sequences, late Pleistocene, Rapolano Terme, Italy. *Sedimentology*, **45**, 163–180, http://dx.doi.org/10.1046/j.1365-3091.1998.00141.x.

Guo, L. & Riding, R. 1999. Rapid facies changes in Holocene fissure ridge hot spring travertines, Rapolano Terme, Italy. *Sedimentology*, **46**, 1145–1158, http://dx.doi.org/10.1046/j.1365-3091.1999.00269.x.

Hancer, M. 2013. Study of the structural evolution of the Babadağ-Honaz and Pamukkale fault zones and the related earthquake risk potential of the Buldan region in SW Anatolia, east of the Mediterranean. *Journal of Earth Science*, **24**, 397–409.

Hancock, P.L., Chalmers, R.M.L., Altunel, E. & Çakir, Z. 1999. Travitonics: using travertines in active fault studies. *Journal of Structural Geology*, **21**, 903–916, http://dx.doi.org/10.1016/S0191-8141(99)00061-9.

Kaymakci, N. 2006. Kinematic development and paleostress analysis of the Denizli Basin (Western Turkey): Implications of spatial variation of relative paleostress magnitudes and orientations. *Journal of Asian Earth Sciences*, **27**, 207–222.

Kele, S., Özkul, M., Gökgöz, A., Fórizs, I., Baykara, M.O., Alçiçek, M.C. & Németh, T. 2011. Stable isotope geochemical and facies study of Pamukkale travertines: New evidences of low-temperature non-equilibrium calcite–water fractionation. *Sedimentary Geology*, **238**, 191–212, http://dx.doi.org/10.1016/j.sedgeo.2011.04.015.

Kerrich, R. 1986. Fluid infiltration into fault zones: Chemical, isotopic and mechanical effects. *Pure and Applied Geophysics*, **124**, 225–268, http://dx.doi.org/10.1007/BF00875727.

Koban, C.G. & Schweigert, G. 1993. Microbial origin of travertine fabrics—two examples from southern Germany (Pleistocene Stuttgart travertines and Miocene Riedijschingen travertine). *Facies*, **29**, 251–264.

Koçyiğit, A. 2005. The Denizli graben–horst system and the eastern limit of the western Anatolian continental extension: Basin fill, structure, deformational mode, throw amount and episodic evolutionary history, SW Turkey. *Geodinamica Acta*, **18**, 167–208, http://dx.doi.org/10.3166/ga.18.167-208.

Martinez-Diaz, J.J. & Hernandez-Enrile, J.L. 2001. Using travertine deformations to characterize paleoseismic activity along an active oblique-slip fault: The Alhama de Murcia fault (Betic Cordillera, Spain). *Acta Geologica Hispanica*, **36**, 297–313.

Mesci, L.B., Gürsoy, H. & Tatar, O. 2008. The evolution of travertine masses in the Sivas Area (Central Turkey) and their relationships to active tectonics. *Turkish Journal of Earth Sciences*, **17**, 219–240.

Mesci, L.B., Tatar, O., Piper, J.D.A., Gürsoy, H., Altunel, E. & Crowley, S. 2013. The efficacy of travertines as a palaeoenvironmental indicator: Palaeomagnetic study of neotectonic examples from Denizli, Turkey. *Turkish Journal of Earth Sciences*, **22**, 191–203, http://dx.doi.org/10.3906/yer-1112-3.

Nelson, S.T., Mayo, A.L., Gilfilan, S., Dutson, S.J., Harris, R.A., Shipton, Z.K. & Tingey, D.G. 2009. Enhanced fracture permeability and accompanying fluid flow in the footwall of a normal fault: The Hurricane fault at Pah Tempe hot springs, Washington County, Utah. *Geological Society of America Bulletin*, **121**, 236–246, http://dx.doi.org/10.1130/B26285.1.

Özkul, M., Kele, S., *et al.* 2013. Comparison of the Quaternary travertine sites in the Denizli extensional basin based on their depositional and geochemical data. *Sedimentary Geology*, **294**, 179–204.

Pedley, H.M. 1990. Classification and environmental models of cool freshwater tufas. *Sedimentary Geology*, **68**, 143–154, http://dx.doi.org/10.1016/0037-0738(90)90124-C.

Pedley, M. 2009. Tufas and travertines of the Mediterranean region: a testing ground for freshwater carbonate concepts and developments. *Sedimentology*, **56**, 221–246.

Pentecost, A. 2005. *Travertine*. Kluwer, Dordrecht.

Person, M., Hofstra, A., Sweetkind, D., Stone, W., Cohen, D., Gable, C.W. & Banerjee, A. 2012. Analytical and numerical models of hydrothermal fluid flow at fault intersection. *Geofluids*, **12**, 312–326, http://dx.doi.org/10.1111/gfl.12002.

Pichler, T. & Veizer, J. 2004. The precipitation of aragonite from shallow water hydrothermal fluids in a coral reef, Tutum Bay, Ambitle Island, Papua New Guinea. *Chemical Geology*, **207**, 31–45, http://dx.doi.org/10.1016/j.chemgeo.2004.02.002.

Pollard, D.D. & Aydin, A. 1988. Progress in understanding jointing over the past century. *Geological Society of America Bulletin*, **100**, 1181–1204, http://dx.doi.org/10.1130/0016-7606(1988)100<1181:PIUJOT>2.3.CO;2.

Rimmelé, G., Jolivet, L., Oberhansli, R. & Goffe, B. 2003. Deformation history of the high-pressure Lycian Nappes and implications for tectonic evolution of SW Turkey. *Tectonics*, **22**, TC901041, http://dx.doi.org/10.1029/2001TC901041.

Rimmelé, G., Oberhansli, R., Candan, O., Goffe, B. & Jolivet, L. 2006. The wide distribution of HP–LT rocks in the Lycian Belt (Western Turkey): Implications for accretionary wedge geometry. *In*: Robertson, A.H.F. & Mountrakis, D. (eds) *Tectonic Development of Eastern Mediterranean Region*. Geological Society, London, Special Publications, **260**, 447–466, http://dx.doi.org/10.1144/GSL.SP.2006.260.01.18.

Rowland, J.V. & Sibson, R.H. 2004. Structural controls on hydrothermal flow in a segmented rift system, Taupo Volcanic Zone, New Zealand. *Geofluids*, **4**, 259–283, http://dx.doi.org/10.1111/j.1468-8123.2004.00091.x.

Şaroğlu, F., Emre, Ö & &boray, A. 1987. *Türkiye'nin diri fayları ve depremselliği*. Scientific Report of the General Directorate of Mineral Research and Exploration of Turkey, **8174**.

Şaroğlu, F., Emre, Ö & &kuşçu, İ 1992. *Active fault map of Turkey, Scale 1:1.000.000*. General Directorate of Mineral Research and Exploration of Turkey, Ankara.

Selim, H.H. & Yanik, G. 2009. Development of the Cambazli (Turgutly/Manisa) fissure-ride-type travertine and relationship with active tectonics, Gediz Graben, Turkey. *Quaternary International*, **199**, 157–163, http://dx.doi.org/10.1016/j.quaint.2008.04.009.

Şengör, A.M.C. 1987. Cross faults and differential stretching of hanging walls in regions of low-angle normal faulting: examples from western Turkey. *In*: Coward, M.P., Dewey, J.F. & Hancock, P.L. (eds) *Continental Extensional Tectonics*. Geological Society, London, Special Publications, **28**, 575–589.

Sibson, R.H. 1987. Earthquake rupturing as a hydrothermal process. *Geology*, **15**, 701–704, http://dx.doi.org/10.1130/0091-7613(1987)15<701:ERAAMA>2.0.CO;2.

Sibson, R.H. 2000. Fluid involvement in normal faulting. *Journal of Geodynamics*, **29**, 469–499, http://dx.doi.org/10.1016/S0264-3707(99)00042-3.

Şimşek, Ş., Günay, G., Elhatip, H. & Ekmekçi, M. 2000. Environmental protection of geothermal waters and travertines at Pamukkale, Turkey. *Geothermics*, **29**, 557–570, http://dx.doi.org/10.1016/S0375-6505(00)00022-5.

Sun, S. 1990. *Denizli-Uşak Arasının Jeolojisi ve Linyit Olanakları*. Scientific Report of the General Directorate of Mineral Research and Exploration of Turkey, **9985**.

Temiz, U. & Eikenberg, J. 2011. U/Th dating of the travertine deposited at transfer zone between two normal faults and their neotectonic significance: Cambazli ridge travertines (the Gediz Graben, Turkey). *Geodinamica Acta*, **24**, 95–105, http://dx.doi.org/10.3166/ga.24.95-105.

Temiz, U., Gokten, E. & Eikenberger, J. 2009. U/Th dating of fissure ridge travertines from the Kirsehir region (central Anatolia, Turkey); structural relations and implications for the neotectonic development of the Anatolian block. *Geodinamica Acta*, **22**, 201–213, doi:10.3166/ga.22.201-213.

ten Veen, J.H., Boulton, S.J. & Alçiçek, M.C. 2009. From palaeotectonics to neotectonics in the Neotethys realm: The importance of kinematic decoupling and inherited structural grain in SW Anatolia (Turkey). *Tectonophysics*, **473**, 261–281, http://dx.doi.org/10.1016/j.tecto.2008.09.030.

Tripp, G.I. & Vearncombe, J.R. 2004. Fault/fracture density and mineralization: A contouring method for targeting gold exploration. *Journal of Structural Geology*, **26**, 1087–1098, http://dx.doi.org/10.1016/j.jsg.2003.11.002.

Uysal, İ.T., Feng, Y., *et al.* 2007. U-series dating and geochemical tracing of late Quaternary travertine in co-seismic fissures. *Earth and Planetary Science Letters*, **257**, 450–462, http://dx.doi.org/10.1016/j.epsl.2007.03.004.

Uysal, İ.T., Feng, Y., Zhao, J., Isik, V., Nuriel, P. & Golding, S. 2009. CO_2 degassing in seismically active zones during the late Quaternary. *Chemical Geology*, **265**, 442–454, http://dx.doi.org/10.1016/j.chemgeo.2009.05.011.

van Hinsbergen, D.J.J. 2010. A key extensional metamorphic complex reviewed and restored: The Menderes Massif of western Turkey. *Earth-Science Reviews*, **102**, 60–76, http://dx.doi.org/10.1016/j.earscirev.2010.05.005.

van Noten, K., Claes, H., Soete, J., Fourbert, A., Özkul, M. & Swennen, R. 2013. Fracture network and strike-slip deformation along reactivated normal faults in Quaternary travertine deposits, Denizli Basin, Western Turkey. *Tectonophysics*, **588**, 154–170, http://dx.doi.org/10.1016/j.tecto.2012.12.018.

Westaway, R. 1990. Block rotations in western Turkey: 1. Observational evidence. *Journal of Geophysical Research*, **95**, 19857–19884, http://dx.doi.org/10.1029/JB095iB12p19857.

Westaway, R. 1993. Neogene evolution of the Denizli region of western Turkey. *Journal of Structural Geology*, **15**, 37–53, http://dx.doi.org/10.1016/0191-8141(93)90077-N.

Westaway, R. 1994. Present-day kinematics of the Middle and Eastern Mediterranean. *Journal of Geophysical Research*, **99**, 12071–12090, http://dx.doi.org/10.1029/94JB00335.

Yanik, G., Uz, B. & Esenli, F. 2005. An example of the fissure-ridge type travertine occurrences: The Cambazli travertine, Turgutlu, west Anatolia. *In*: Özkul, M., Yagiz, S. & Jones, B. (eds) *Proceedings of 1st International Symposium on Travertine, September 21–25, 2005, Denizli, Turkey*. Kozan Ofset, Ankara, 149–153.

Yilmaz, Y., Genç, Ş.C., Gürer, F., Bozcu, M., Yilmaz, K., Karacik, Z., Altunkaynak, Ş. & Elmas, A. 2000. When did the western Anatolian grabens begin to develop? *In*: Bozkurt, E., Winchester, J.A. & Piper, J.D.A. (eds) *Tectonics and Magmatism in Turkey and the Surrounding Area*. Geological Society, London, Special Publications, **173**, 353–384.

Received 26 March 2013; revised typescript accepted 3 November 2013.
Scientific editing by Erdin Bozkurt.

The Geological Society

serving science & profession

Lyell Collection

Geological Society publications online

The Lyell Collection

One of the largest integrated collections of online Earth science literature in the world

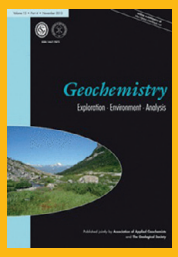

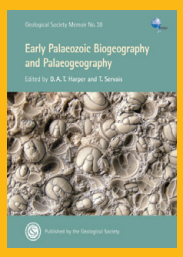

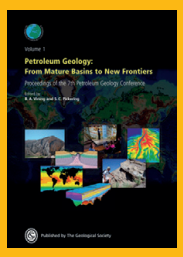

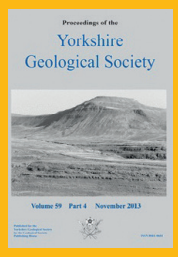

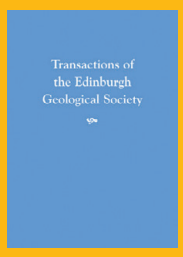

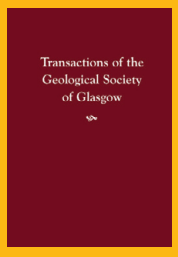

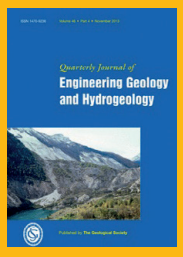

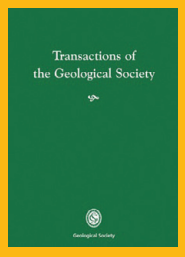

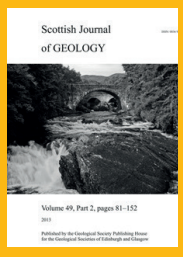

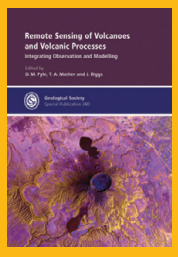

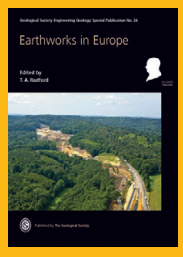

What is the Lyell Collection?

The Lyell Collection is an online collection comprising the Society's journal titles, Special Publications and key book series. Cutting edge science sits alongside important historical material, benefiting from the superb functionality offered by the online host, HighWire Press.

With 260,000 peer-reviewed pages, 26,000 articles and 1,000 volumes, the Lyell Collection is an invaluable tool for the researcher and student alike.

- Full text in HTML and PDF format
- Actively linking to cited references
- Free abstracts
- Free ETOC alerting
- Selected articles free online
- The Lyell Collection welcomes Open Access papers
- JGS, QJ, GEEA and PG offer specially-designed sites for those using mobile devices
- New: Transactions of the Edinburgh Geological Society and Transactions of the Geological Society of Glasgow

Special Publication archives

The first 300 volumes of the Geological Society's Special Publications Online Archive are available as a one-off purchase with perpetual access.

The Geological Society

The Geological Society of London was founded in 1807 and is the UK national society for geosciences. It is a global leader in Earth science publishing, dedicated to providing high-quality content and service throughout the world.

GEOFACETS™

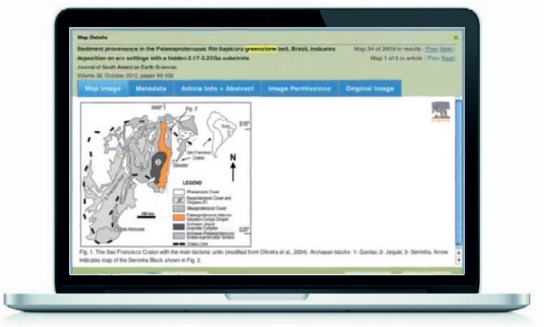

Geofacets-GSL Millennium Edition

Elsevier and the Geological Society of London (GSL) have collaborated to provide GSL members with a unique opportunity to gain individual access to 24,000+ geological maps from the renowned Lyell Collection through the Geofacets platform.

The Geofacets platform is an innovative map-based research tool designed for geoscientists. These maps are downloadable, geo-referenced, and accompanied by metadata, article abstracts and links to original source articles.

bp

Foundation Sponsor

For more information visit www.lyellcollection.org